Università di Foggia
Medicina Clinica e Sperimentale

PhD Thesis in Basic and Clinical Neuroscience
Cycle XXXVIII

Circadian clockwork dysfunction in cancer: from molecular characterization to chronotherapeutic vulnerabilities

Tutor
Prof. Claudia Piccoli

PhD Candidate
Aristide Ferrante

Academic year 2024/25

Ai miei genitori,
testimoni di ogni passo
di questo viaggio

Abstract

Circadian rhythms have emerged in recent years as key regulators of several cancer hallmarks, such as enhanced proliferation, metabolic rewiring and drug resistance. Circadian disruption is in fact closely linked to cancer initiation and progression, thus there is a growing interest in understanding how the molecular clock can influence oncogenesis. Cancer stem cells (CSCs) in particular display a peculiar circadian disruption, suggesting how the lack of clockwork functionality could be a key factor in conferring self-renewal, metastatic and drug resistance phenotypes.

This study aimed to investigate how circadian rhythm alterations affect proliferation and metabolism, in the sake to unveil the contribution of the clock to CSCs survival and drug response, uncovering potential therapeutic vulnerabilities.

The circadian phenotype of Differentiated and CSCs from bladder cancer, osteosarcoma and breast cancer was characterized using molecular biology and biochemical approaches, unveiling a profound alteration and downregulation of cell-autonomous circadian oscillations present in the differentiated counterparts. A robust proliferation rate circadian pattern emerged in differentiated cancer cells, that was in turn abrogated in CSCs; pharmacological modulation of core clock genes was able to induce a cytotoxic response in differentiated cancer cells, while the clock deregulation rendered CSCs refractory to clock-inducing drugs.

The lack of clock control over metabolism was reflected by uncontrolled and aberrant swings in the glycolytic activity, resulting in a plastic bioenergetic phenotype displayed by CSCs.

The present study confirmed the profound alterations of clockwork functionality in CSCs and how they impact cell proliferation and metabolic rewiring, as well as conferring resistance to possible chronotherapeutic interventions. More studies are needed to understand how to potentially combine chronotherapy and conventional chemotherapy in order to eradicate CSCs.

INDEX

1 INTRODUCTION

1.1 Circadian rhythms

Numerous physiologic and behavioural processes are tightly linked to the environmental changes dictated by the alternation of daylight and nighttime, which are a direct consequence of earth's rotating motion[1]. Almos all living organisms have evolved ways to adapt and anticipate these changes, developing what we now refer to as circadian rhythms[1,2].

In mammals, where the main synchronizing cue is the exposure to light, the endogenous circadian system has a preponderant role in regulating the sleep-wake cycle, hormonal fluctuations, temperature changes, feeding-fasting cycles, and enables the organism to adapt to the 24h daylight/nighttime cycle in the optimal fashion[1]. In humans the circadian clock is organized in a hierarchical system, composed by a central pacemaker identified in a small subset of hypothalamic nuclei, a region named the Suprachiasmatic Nuclei (SCN): these neurons receive photic signals from the melanopsin-expressing retinal ganglion cells (ipRGCs) through the retino-hypothalamic tract belonging to the optic nerve (Figure 1) [3].

The central clock then sends a plethora of signals to the peripheral clocks present in each cell and tissue, allowing the synchronization, coordination and integration between external conditions and organism functions[3]. The main example of the aforementioned phenomenon is the SCN regulation of the rhythmic and cyclic melatonin secretion by the pineal gland in dark conditions, which will then induce relax and drowsiness; in an antiphasic fashion, the SCN will promote cortisol secretion during daylight exposure, which will in turn favour wakefulness and focus, required for diurnal activities[1].

However, peripheral clocks can be also influenced by other external stimuli, such as food intake, temperature changes and physical exercise, that will then influence the oscillation of hormonal, metabolic and behavioural functions in order to properly respond to the initial

synchronizing cue[4]. Endogenous physiologic signals are also able to influence both central and peripheral clocks through neural and hormonal feedbacks mechanisms[1].

All together, these tissue-specific oscillations last around 24 hours, herby the name circadian rhythms, from the latin "*circa diem*", translated as "about one day"[5].

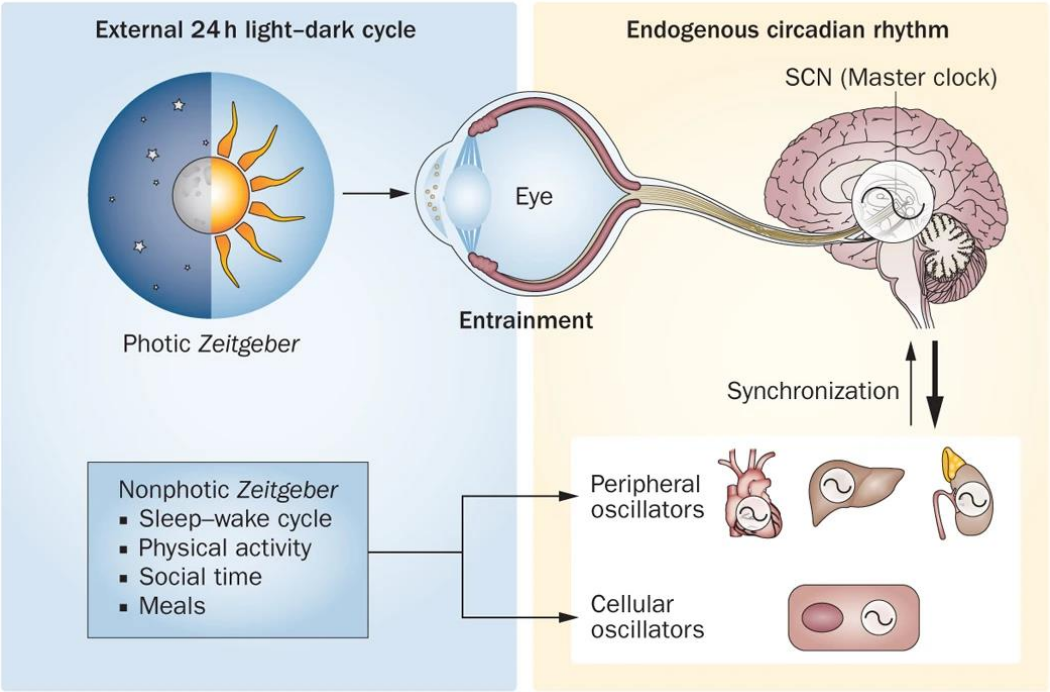

Figure 1 Schematic representation of the central and peripheral clock systems and the various types of synchronizing cues[6].

1.1.1 The molecular clock

At the molecular level both the central and peripheral clocks revolve around a finely tuned transcriptional-translational feedback loop (TTFL), which constitutes a cell-autonomous molecular clock machinery, that then dictates the rhythmic expression of genes involved in metabolic, cell cycle, biosynthetic and signal transduction pathways[6].

The two main *Core Clock Genes* (CCG) are the Aryl hydrocarbon receptor nuclear translocator-like 1 (*ARNTL1*) gene and the Circadian locomotor output cycles kaput (*CLOCK*) gene, which are encoding for the two transcription factors BMAL1 and CLOCK: the heterodimerization of the two proteins provokes the activation of the BMAL1/CLOCK complex, that

translocates inside the nucleus, binds to E-box sequences (5'-CACGTG-3' o 5'-CACGTT-3') present in the promoter regions of target genes thanks to the basic Helix-Loop-Helix (bHLH) structure of the BMAL1 protein, thus activating the expression of the Period (Per1, Per2, Per3) and Cryptochrome (Cry1, Cry2) proteins (Figure 2) [7]. The Per and Cry proteins can then heterodimerize and inhibit BMAL1/CLOCK activity, hereby forming a primary regulatory feedback loop (Figure 2)[8,9]. The half-life of these protein are crucial for the regulation of the period of the endogenous cell-autonomous oscillations: the Casein kinase 1 CK1δ/ε and AMPK are involved in the phosphorylation and consequent degradation of Pers and Crys respectively[10–13].

BMAL1/CLOCK also promote the expression of a set of factors that belong to the secondary feedback circuitry, that are Retinoic acid-related Orphan Receptors (Rorα, Rorβ, Rorχ), and the orphan nuclear receptor Rev-Erbα Rev-Ervβ (Figure 2). Ror proteins are transcription factors that bind to the that positively regulate BMAL1 expression by binding to the *Retinoic Acid-Related Orphan Response Element* (RORE) found within the *ARNTL1* promoter region, while Rev-Erbα and Rev-Ervβ are able to repress BMAL1 expression by antagonizing Ror proteins at the level of RORE sequences[4,5,14,15]. Overall the secondary feedback loop is responsible for the amplitude and robustness of the oscillations regulated by the molecular clock.

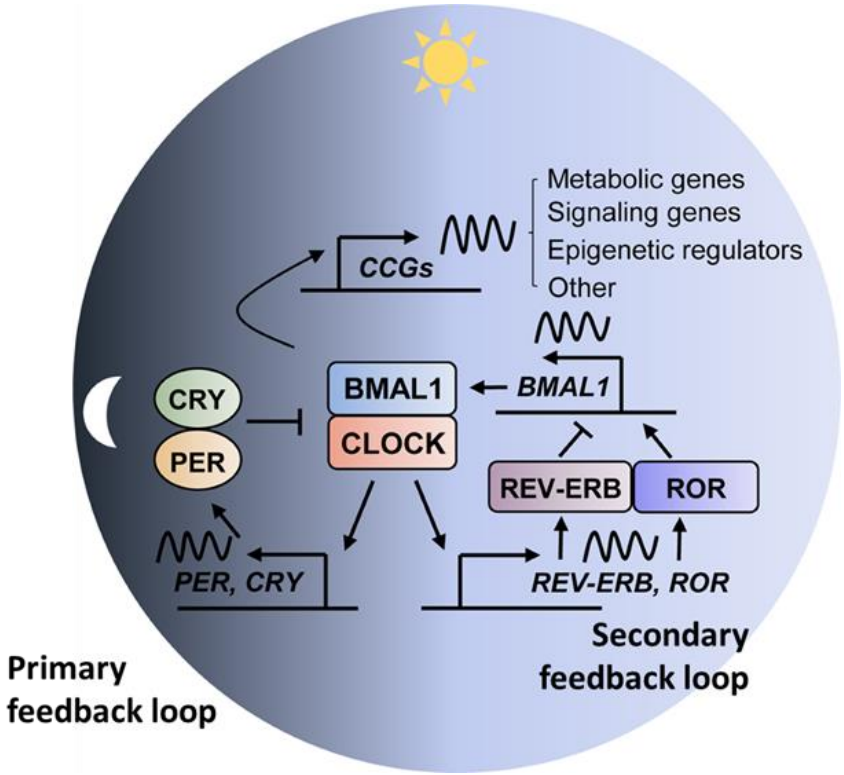

Figure 2: The molecular clock[1].
Schematic representation of the Transcriptional-Translational Feedback Loop. The BMAL1/CLOCK heterodimer promotes the transcription of its own repressors Pers and Crys in a primary feedback loop. The Ror and Rev-Erb proteins, members of the secondary feedback loop, will positively and negatively modulate the BMAL1 protein expression. Overall the TTFL will also regulate a plethora of metabolic, signalling and epigenetic genes.

The intertwining between the rate of transcription, translation, post-translational modifications and protein turnover of the various actors belonging to the CCG determines the 24h fluctuation cycles regulated by the circadian machinery at the molecular and cellular level[4]. There are, however, other mechanisms in play which have not been studied yet in the same extent as the circadian system, such as the *ultradian rhythms*, that seems to be governed by systems independent of CCG function, like the Xbp-1u protein[16].

1.2 The role of circadian clock in physiology and pathophysiology

From 1950s onwards a large body of studies have highlighted the importance of light exposure and its impact on the circadian system and on physiologic processes in numerous living organisms[17]. The retinal ganglion cells not only sends signal to the SCN, but also display projection to brain regions involved in metabolic regulation, such as the the sub-paraventricular zone (sPVZ), the paraventricular nucleus of the hypothalamus (PVH), while also indirectly reaching the dorsomedial hypothalamus (DMH), the arcuate nucleus (ARC)[18,19].

Hereby, it is clear the existence of a strong connection between circadian clock synchronization with external cues and the orchestration of the whole organism functions. Therefore, the misuse of artificial light, shift work, jet-lag and other insults to the physiologic day/night cycle can jeopardize not only circadian function, but can in turn compromise the optimal function of multiple organs and tissues. The disruption of the synchronization between internal clocks and external cues can result in sleepiness, fatigue, digestive problems, irritability, to the point of even increase the risk for cardiovascular disease, metabolic syndrome or cancer[20–22].

1.2.1 Circadian clock influence on metabolism

The circadian control over metabolism is well documented, while its molecular mechanisms remain less understood. Glucose levels and insulin sensitivity are known to vary at different times of the day, and it is known that the circadian hormone melatonin can regulate insulin secretion during nighttime[23,24]. Rodent studies have uncovered that loss in rhythmic oscillations of glucose metabolism can lead to development in type 2 diabetes.

Mice with an altered sleep-wake cycle display impairment in glucose tolerance and an inversion in normal clock gene expression[25]. *Clock* gene mutation (*Clock-Δ19*) carrying mice display weak behavioural rhythms,

arrhythmic expression of metabolic genes in key organs like liver, muscle and pancreas, resulting in compromised glucose and lipid homeostasis, as well as in diet-induced obesity[26–28]. Loss of Bmal1 gene causes similar abruption in locomotor activity, adipogenesis, hepatic glucose and carbohydrate metabolism[29–31]. Disruption of primary feedback loop members such as PER2 proteins often result in altered insulin sensitivity, hypoglycemia, obesity, while CRYs knout leads to increased expression of gluconeogenic genes, as well as increased hepatic glucose production[32–34].

In a similar fashion, mutations in various TTFL and *Clock Controlled Genes* often result in impairments of lipid metabolism, ranging from hypertriglyceridemia to lipid accumulation or malabsorption, leading to , mainly due to the disruption of liver and intestine function[27,28,35,36].

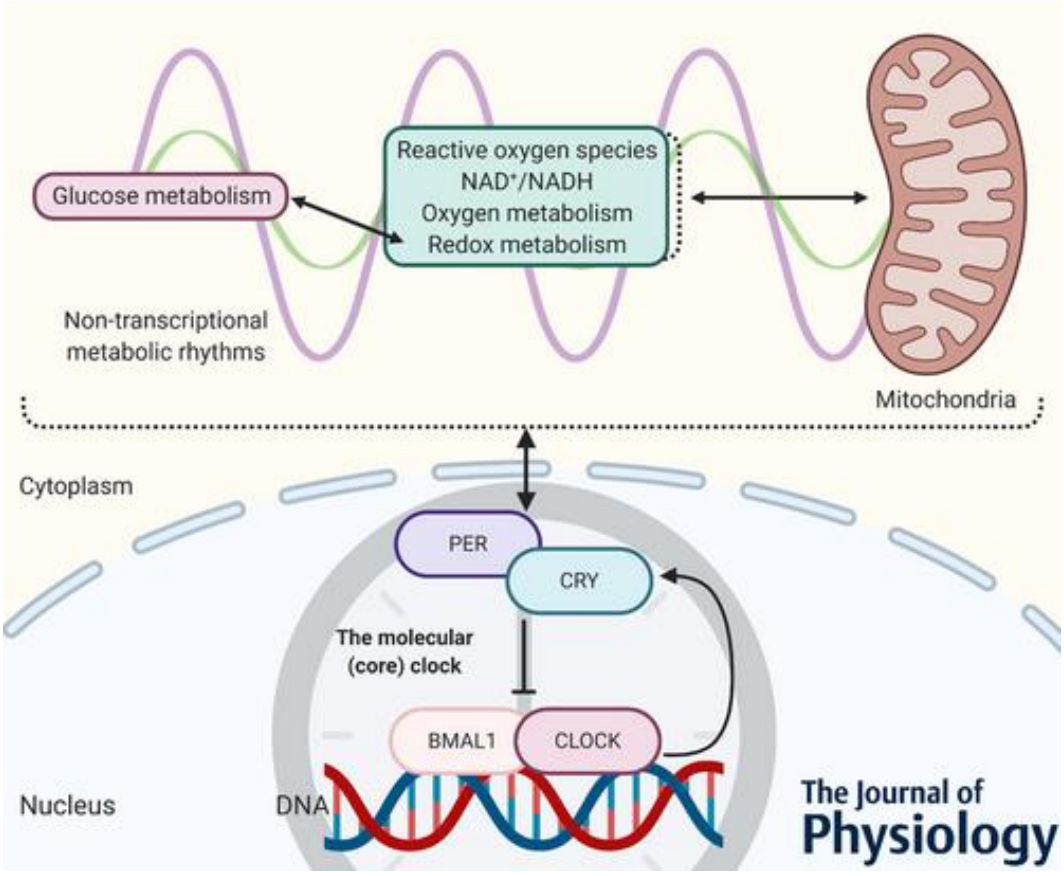

Figure 3. Schematic representation of the interplay between circadian clock and metabolism[37].

1.2.2 Clock control over cellular and mitochondrial metabolism

Mitochondria are pivotal elements in the regulation of several key cellular processes, ranging from metabolic and energetic control to calcium homeostasis and apoptosis regulation. From a metabolic point-of-view, mitochondria harbour numerous fundamental processes such as the TCA cycle, fatty acids oxidation and ATP production thanks to oxidative phosphorylation (OXPHOS) carried out by the respiratory chain complexes and ATP Synthase[37].

Mitochondria also are dynamic organelles: Damaged mitochondria undergo a process known as fission, allowing their degradation, a process named mitophagy, essential for the mitochondrial quality control. These events are closely intertwined with the biogenesis of new mitochondria and the consequent fusion of the newly formed organelles into the pre-existing mitochondrial network[38].

Chromatin immunoprecipitation (ChIP)-sequencing dataset for Bmal1, Clock, and Cry highlighted 211 mitochondrial-related genes as targets, including OXPHOS complexes, TCA cycle, mitochondrial dynamics and β-oxidation related genes, suggesting that these processes are under control of the molecular clock[39,40]. Moreover several nuclear-encoded mitochondrial proteins are dysregulated in Clock mutant mice, while the correlation between the oscillations of the mitochondrial transcriptome and proteome showed only mild significance, pointing toward post-translational modifications as an important crossroad in the circadian control over mitochondrial function[41]: in particular acetylome analysis of TCA cycle proteins showed a CLOCK-dependent profile, and Bmal1 KO animals alters mitochondrial proteins acetylation status[42–44].

It has been demonstrated how the utilization of nutrients by mitochondria changes during the day: the mitochondrial fatty acid importer Carnitine palmitoyltransferase 1 (CPT1) displays oscillations that result in rhythmic performance of respiratory activity[41]. Another key enzyme in the regulation of substrate utilization in mitochondria is the pyruvate dehydrogenase, which exhibit a circadian-dependent alternation between

phosphorylated/unphosphorylated statuses, thus leading to the rhythmicity in the oxidation of pyruvate[40,41]. Mitochondrial respiration has been shown to display a clock-dependent rhythmic oscillatory profile in mice liver and in cell lines[40,43,45,46], and various mechanisms have been proposed to unveil the clock-mitochondria relationship, many of which point toward the circadian clock-NAD+ axis: NAMPT, the rate limiting enzyme in the NAD+ biosynthesis, is under circadian control, leading to the oscillation of NAD+ content, as well as oxygen consumption rate (OCR) and fatty acids oxidation. Clock-driven NAD+ dependent deacetylase SIRT3 dictates protein acetylation status inside the mitochondrial matrix, governing the activity of enzymes and respiratory chain activity[43,46]. Another key regulator in the interplay between clock machinery and mitochondrial metabolism is AMP-activated protein kinase (AMPK), known to be the cellular energetic sensor, which phosphorylates its targets upon drop of the ATP/AMP ratio. One of the targets of AMPK is the master regulator of mitochondrial biogenesis Peroxisome proliferator-activated receptor gamma coactivator 1-α (PGC-1α), which is activated upon phosphorylation. AMPK is also able to activate mitochondrial fission and mitophagy via mitochondrial fission factor (MFF) and ULK1 respectively[47].

Mitochondrial dynamics have also been shown to be controlled by circadian machinery: the fusion of mitochondrial network peaks coincidentally with the increase in ATP content and OXPHOS[48–50]. This phenomenon is coordinated by the circadian-driven expression of proteins that regulate fusion Mitofusin-1 (MFN1) Mitofusin-2 (MFN2) and Optic Atrophy 1 (OPA1), and fission Dynamin related protein 1 (DRP1)[40,48]. Notably, post-translational modification in Drp1 (de-activating phosphorylation at Ser637) displays a 24h oscillation pattern[48]. Clock dysfunction also results in abruption of rhythmic expression of mitochondrial fission and mitophagy proteins, highlighting the prominent role of circadian clock in the regulation of mitochondrial morphology changes[40].

The mechanism that feeds back from the mitochondria to the molecular clock is still poorly understood. Pharmacological inhibition of

OXPHOS and depletion in mtDNA copy number causes strong disruption of the clock gene expression[51].

1.3 Circadian system deregulation in cancer

Recent evidences have brought attention to the role of circadian rhythms dysfunction and its association with increased risk of developing cancer[52]. With the rapid industrialization and advancement of modern society, an increasing proportion of the global population frequently experiences disruptions to their circadian rhythms due to lifestyle factors such as shift work, jet lag, exposure to artificial light at night, and irregular sleep–wake patterns[1]. Approximately 80% of the global population is exposed to light during nighttime hours, and about 18–20% of the workforce in the United States and Europe engages in night or shift work. Such circadian misalignments are associated with an increased risk of cancer, and these evidences led the International Agency for Research on Cancer (IARC) to classify "shift-work that involves circadian disruption" as potentially "carcinogenic to humans (Group 2A)" in 2007 and again in 2019[53]. Animal studies demonstrated that Chronic jet-leg induced circadian dysfunction promoted tumor growth and progression thanks to accelerated tumor cell cycle progression and growth rate[1]. Moreover circadian disruption promotes metastasis in a breast cancer mouse model by increasing stemness and tumor-initiating potential of cancer cells[1].

Molecular clock and cancer hallmarks

Molecular clock has a prominent role in the regulation of the cell cycle, DNA repair, apoptosis, senescence, autophagy, and other oncogenic and immune pathways. The circadian disruption can lead to uncontrolled cell proliferation, evasion of apoptosis, metastatic dissemination, immune escape, enhanced angiogenesis, and resistance to anticancer therapies — all recognized hallmarks of cancer[1]. Silencing of Bmal1 and/or Clock has been shown to promote tumor growth and proliferation across several cancer types, including hematologic malignancies, colorectal cancer, pancreatic cancer, tongue squamous cell carcinoma (TSCC), breast cancer, lung

adenocarcinoma, hepatocellular carcinoma (HCC), nasopharyngeal carcinoma (NPC), and glioblastoma (GBM), while the over-expression of circadian activators can suppress malignant phenotype via cell cycle arrest and p53-dependent induction of apoptosis[1]. Notably, up regulation of PER1/2 has been linked to tumor suppression, possibly via the inhibition of PI3K/AKT/mTOR pathway and cell cycle arrest[54,55]. Primary feedback loop members CRY1/2 have also been proposed as tumor-regulating factors by promoting cMYC and E2F degradation[56]. These evidences have also been validated by a large-scale analysis that unveiled the down-regulation of PERs and CRYs among 32 human cancer types, indicating their role as tumor suppressor factors[57].

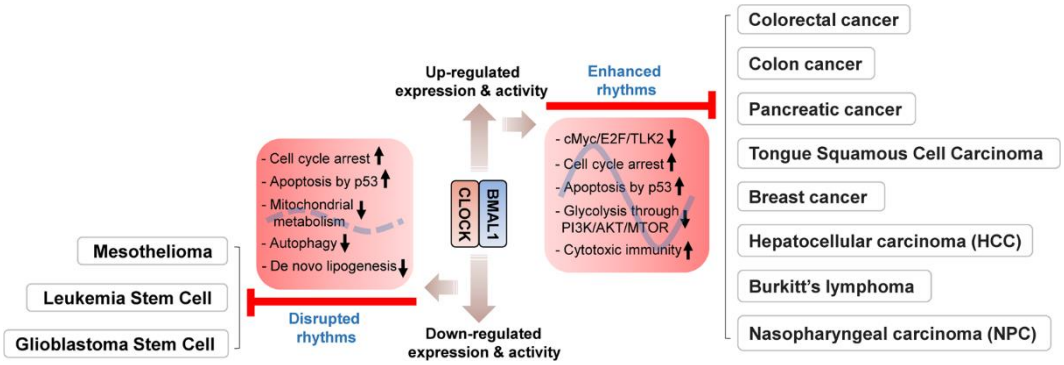

Figure 4. Schematic representation of clock alterations in different cancer types

Other CCG members have been shown to have tumor promotive function depending on the cancer type: BMAL1 knockdown can induce increased apoptosis and cell cycle arrest in mesothelioma and cancer stem cells (CSCs) derived from GBM or acute myeloid leukemia[1]. Moreover, BMAL1 O.E. can promote invasion and metastasis in breast cancer models[58]. CRY1 has been suggested to be behave as an oncogenic factor by promoting DNA repair in tumors. Also Cry1/2$^{-/-}$ mouse model displays enhanced apoptosis following UV or cisplatin induced DNA damage[59]. Further investigations have demonstrated the tumor-promoting role of CRY1, revealing how the TTFL member facilitates the degradation of the

tumor suppressor p53 through modulation of its interaction with the E3 ubiquitin ligase MDM2 proto-oncogene in bladder cancer cells[60].

Overall the role of the clock in oncogenesis, tumor progression and metastasis remains to be fully elucidated.

Molecular clock and cell cycle regulation

A growing body of evidences is pointing to the role of CCG in the regulation of cell cycle progression, as TTFL components have been identified as transcriptional regulators of critical proteins involved in checkpoints advancement.

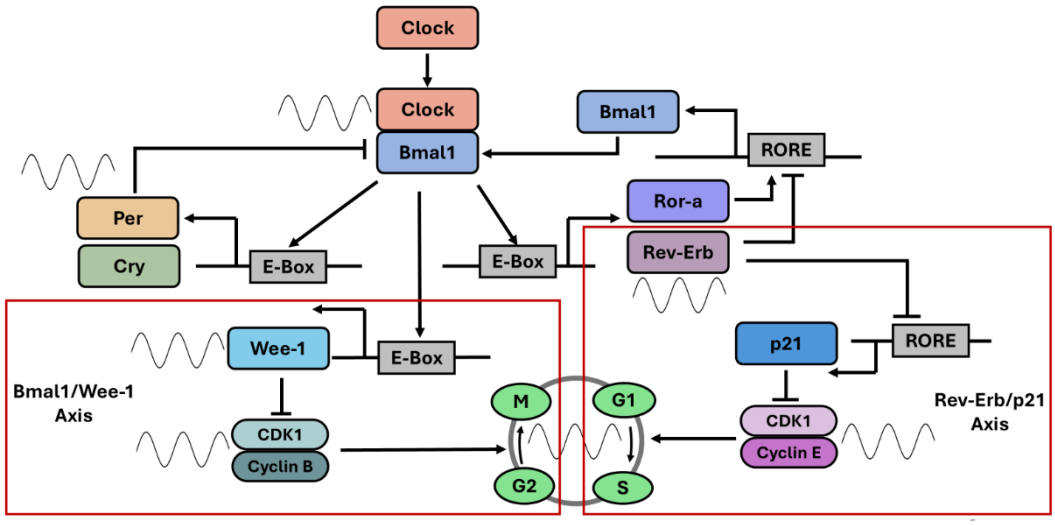

Figure 5. Schematic representation of the pathways linking the molecular clock to the cell cycle.

Two main ways are known in which the clock can interact with the cell cycle: the first one is the Bmal1-induced expression of the kinase Wee1, that in turn can inhibit CDK1/Cyclin B, therefore blocking the G2/M checkpoint progression (Figure 5)[61]. The second pathway involves the negative regulation exerted by Rev-Erbα on the expression of the G1/S checkpoint inhibitor p21 (Figure 5)[62]. Other TTFL members have a role in the regulation of DNA repair, such as the CRY1 mediated activation of ATR/CHK1 or the PERs interaction with ATM/CHK2 in case of DNA double strand break[63–65].

Circadian machinery can also interact with tumor suppressor genes: p53 can negatively regulate PER2 expression[66]. PER2 can also directly

interact with p53, leading to the enhanced expression of target genes like p21[67]. The oncogene c-MYC is also regulated transcriptionally by Bmal1/NPAS2, while Cry2 promotes its degradation[68,69]. In turn, c-MYC can influence clock function by upregulating Rev-Erbα, thereby inhibiting Bmal1 expression, or by directly suppressing its expression by acting together with the transcription factor MIZ1[70,71].

Altogether these evidences highlight the role of the circadian clockwork as a cancer gatekeeper, governing multiple key cancer hallmarks, and its deregulation could be a crucial step for tumour cells to bypass in order to achieve malignancy.

1.4 Cancer Stem Cells

Tumor heterogeneity refers to the presence of genetically, epigenetically, and phenotypically distinct subpopulations of cancer cells that coexist both between different patients (inter-tumor heterogeneity) and within the same neoplasm (intra-tumor heterogeneity)[72]. Intra-tumor diversity arises from clonal evolution driven by mutations and selective pressures, as well as from microenvironmental influences such as hypoxia, stromal interactions, and immune infiltration[73]. Furthermore, cancer cell plasticity enables phenotypic transitions that enhance adaptability to stress and therapeutic challenges[72].

Cancer stem cells (CSCs) represent a rare and highly tumorigenic subpopulation within malignant tissues that possess the defining properties of self-renewal, differentiation, and tumor initiation[72,73]. In particular, therapeutic resistance belonging to CSCs is one of the main driver of cancer relapse and treatment failure, thus the development of targeted therapies to eradicate CSCs are considered an unavoidable hurdle in the void to eliminate tumor recurrence[74].

1.4.1 Cancer stem cell profile

CSCs are thought to be the basis of oncogenesis and are commonly considered the "tumor initiating cells"[75]. One fundamental peculiarity of CSCs is their capability to maintain an undifferentiated state through self-renewal, having at the same time an elevated differentiation potential, allowing the tumor to preserve a stem cell reservoir, while also generating an heterogeneous progeny of differentiated cancer cells[76].

Two different model have been proposed to explain the origin of CSCs, a hierarchical model and a stochastic model: in the first one CSCs are at the pinnacle of tumor hierarchy and can generate each single subclone belonging to the neoplastic mass, being in this way the root of the disease; the second model infers that tumors originates from the accumulation of casual mutations in normal cell, and CSCs originates from the intratumoral phenotypic heterogeneity[77]. Other evidences suggest that CSCs could originate from malignant transformation of tissue-residents stem/progenitor cells, or from events such as cell-cell fusion between differentiated cancer cells and non-malignant stem cells[78].

From a signalling and molecular point of view, CSCs exhibit a distinct set of features that sustain their stem-like phenotype. Central to CSCs biology are the developmental signalling pathways that regulate stemness in normal tissues but become aberrantly activated in cancer, such as the Wnt/β-catenin pathway, which promotes transcription of pluripotency genes such as NANOG, SOX2, and OCT4, maintaining an undifferentiated state[73]. Another pathway involved in CSCs development is the Notch pathway, which governs asymmetric division and cell-fate determination, while Hedgehog (Hh) signalling sustains proliferation and resistance to differentiation cues[72]. Additionally, PI3K/Akt/mTOR and STAT3 cascades enhance survival, metabolic adaptation, and protection against apoptosis, integrating extrinsic signals from the tumor microenvironment [79]. Crosstalk between these pathways generates a robust, plastic signalling network that enables CSCs to foster tumor growth while maintaining their intrinsic pluripotency.

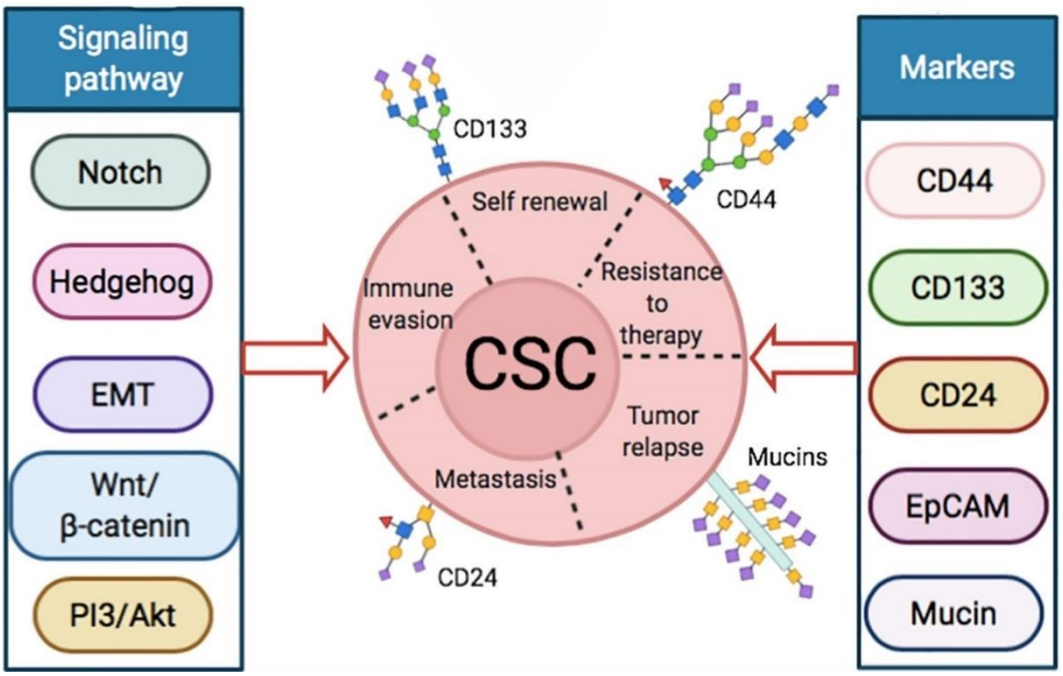

Figure 6. Cancer stem cells markers and signalling pathways[80].

At the molecular level, CSCs are characterized by the expression of specific surface markers, which may vary among tumor types, but can be useful identifiers for CSC isolation and functional assays. One of the most commonly reported markers include CD44, a membrane receptor associated with increased proliferation, self-renewal, tumor initiation and metastatic potential, found to be present in numerous CSCs belonging to different cancer types, including colorectal, breast and gastric cancers[80].

The biomarker CD133 (Prominin-1), is known to be expressed on human Embryonic Stem Cells (hESCs) and only rarely found in normal cells, and it is an established marker for CSCs characterization and isolation. It has been found in breast, liver, stomach and colon cancers, and CD133+ cells display high tumorigenicity and spheroid forming ability, which are also common CSCs features[80]. Overall the presence of this marker is

associated with high cell malignancy and poor overall prognosis in colorectal and breast cancer[80].

ALDH1 is another key CSC marker, which is an enzyme that mediates detoxification and correlates with enhanced self-renewal and resistance to chemotherapy[73].

1.4.2 Metabolic rewiring in CSCs

Metabolic reprogramming refers to the alteration of metabolic pathways in cancer cells compared with their normal counterparts, enabling the acquisition of a metabolic phenotype that supports uncontrolled growth and survival. Such reprogramming ensures a continuous supply of energy and biosynthetic precursors required for the proliferation and maintenance of both cancer cells and cancer stem cells (CSCs)[81]. The enhanced proliferative and metastatic potential observed in malignant cells reflects profound metabolic dysregulation.

In 1924, Otto Warburg first reported the increased reliance of cancer cells on aerobic glycolysis—a phenomenon now known as the Warburg effect—whereby tumor cells preferentially metabolize glucose through glycolysis even in the presence of sufficient oxygen[82,83]. In normal cells, glucose is converted to pyruvate via glycolysis, which is then imported into the mitochondria and oxidized through the tricarboxylic acid (TCA) cycle coupled with oxidative phosphorylation (OXPHOS) to generate adenosine triphosphate (ATP). Warburg demonstrated that, unlike normal cells, the growth of cancer cells predominantly depends on glycolytic ATP production, reflecting a fundamental shift in energy metabolism[82].

We now know that this metabolic reprogramming not only tackles the glycolytic flux activity, but affects amino acids and fatty acids metabolism as well, processes that require mitochondrial bioenergetics to be rewired in order to occur.

Glucose metabolism

Glucose is the main energy source in cancer cells, and its metabolism is the better characterized among tumors. Normal cells oxidize glucose to

carbon dioxide to produce energy through mitochondrial metabolism and oxidative phosphorylation, but tend to switch to lactate production from glucose in case of oxygene depleted conditions (anaerobic glycolysis)[82]. In contrast to this scenario, cancer cell prefer to utilize glycolysis as the main energy producing-flux even in presence normal oxygen conditions, and CSCs have even higher rates of glycolytic activity[84]. To optimize glucose uptake and utilization, cancer cells display high levels of glucose transporter-1 (GLUT-1) and key glycolytic enzymes hexokinase-1 (HK-1) and 2[81].

CSCs usually have increased glucose uptake and have preferential glucose use in numerous cancer types, such as hepatocellular carcinoma. Breast cancer CSCs have been found to have high pyruvate kinase and lactate dehydrogenase (LDH) activity. However in cells where the mitochondrial content is elevated, such as glioma cells, the glycolytic rate is lower, as well as glucose consumption[81].

Mitochondrial metabolism

In normal cells more than 90% of ATP comes from mitochondrial activity. Due to mitochondrial dysfunction, OXPHOS is often suppressed in most CSCs, while the upregulation of mitochondrial respiration is a process linked to epithelial-mesenchymal transition and metastasis[81].

Modulation of mitochondrial metabolism has been proposed as a therapeutic approach in cancer: dichloroacetate (DCA), an inhibitor of pyruvate dehydrogenase kinase (PDK), can enhance the pyruvate dehydrogenase (PDH) activity and promote the production of Acetoacetyl coenzyme A (Acetyl-CoA) from the glucose-derived pyruvate, hereby shifting the cellular metabolism from glycolysis to OXPHOS, leading to reduced cell proliferation in glioblastoma[85]. DCA can also induce ROS production and mitochondrial depolarization in CD133+ glioblastoma cells both *in vitro* and *in vivo*[86].

Mitochondria is the major source of intracellular ROS, which are also known to be second messenger in signaling cascades regulating cell migration, proliferation, stemness maintenance and differentiation[81]. In

normal conditions, ROS production is balanced by the cellular antioxidants systems, and an imbalance in the fine equilibrium between the two can cause oxidative stress, DNA damage and tumorigenesis[87]. Breast cancer stem cells display higher ROS scavenging capabilities due to high antioxidant enzymes expression such as superoxide dismutase, catalase and glutathione peroxidase[88].

Glutamine metabolism

Glutamine is a non-essential amino acid required for cell proliferation, being not only substrate for hexosamine and nucleic acid synthesis, but can also be used as a carbon source to produce energy through the TCA cycle in hypoxic conditions, as it is converted to glutamate by the action of glutaminase and then to α-ketoglutarate[81]. Glutamate can also be used for glutathione (GSH) synthesis, an important reducing agent used to maintain cellular redox balance[81].

The CD44 present in CSCs can interact with the glutamate cystine transporter xCT (SLC7A11), thus promoting GSH synthesis and ROS scavenging potential in gastrointestinal CSCs. The overexpression of the xCT transporter is a common feature in various cancer cell types, including breast, hepatocellular carcinoma and colorectal cancer. High expression of the transporter is also a poor prognosis in lung cancer, while its downregulation reduces proliferation and invasion potential in non-small

cell lung cancer. Finally xCT regulates the expression of stem cell markers, such as Nanog and Sox-2 in glioma cells.

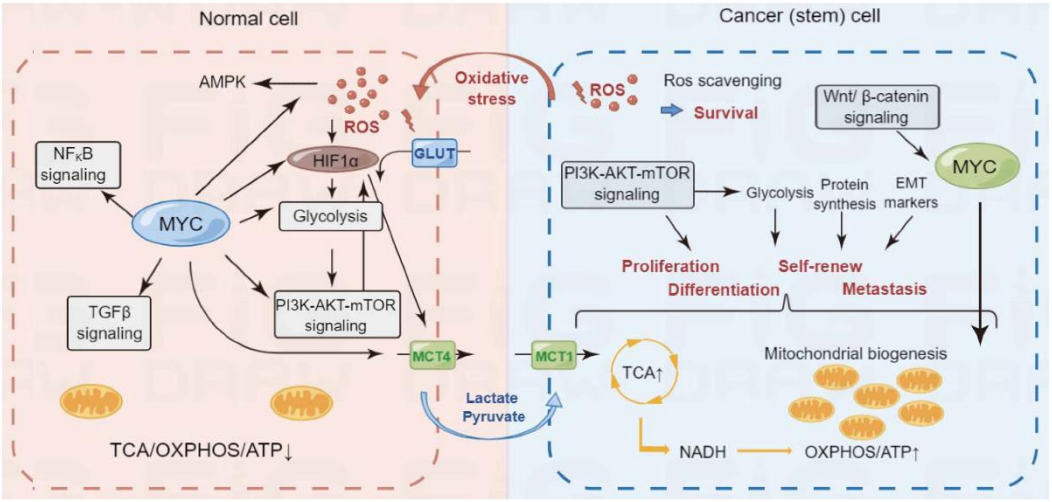

Figure 7. Metabolic rewiring in CSCs[81].
Cancer stem cells exhibit high glycolytic activity, as well as increased glutamate and fatty acid (FA) catabolism, thereby supplying additional metabolic intermediates to the tricarboxylic acid (TCA) cycle and supporting enhanced ATP production. Key metabolic reprogramming pathways, including the PI3K–AKT–mTOR signaling axis, play a central role in sustaining these metabolic shifts and have emerged as promising targets for cancer-directed therapeutic interventions[81]. OXPHOS: oxidative phosphorylation; NADH: nicotinamide adenine dinucleotide reduced form; NAD: nicotinamide adenine dinucleotide; ROS: reactive oxygen species; EMT: epithelial–mesenchymal transition; GLUT: glucose transporter; MCT1: monocarboxylate transporter 1; MCT4: monocarboxylate transporter

Lipid metabolism

Fatty acid (FA) metabolism is another key pathway required for cancer growth, as the carbon chain can be oxidized in mitochondria in a process called fatty acid oxidation (FAO). FAO is regulated by the carnitine palmitoyltransferase 1 (CPT1) enzyme, which regulates the entrance of activated fatty acids (Acyl-CoA) into the mitochondrial matrix[89]. The final product of FAO is Acetyl-CoA, which can be oxidized by the TCA cycle to produce ATP[89].

In CSCs the levels of unsaturated fatty acids is elevated, and there is a high expression of key enzymes involved in FA synthesis, such as citrate lyase, acetyl CoA carboxylase and fatty acid synthase, which are regulated by the lipogenic transcription factor (SREBP1c). Additionally the fatty acid transporter CD36 is also upregulated in CSCs[81].

The mevalonate pathway, required for cholesterol and steroid hormones synthesis, seems also to be involved in CSCs homeostasis. Hydoxymethylglutaryl CoA (HMG-CoA) reductase is the rate limiting enzyme in mevalonate pathway, which has been found to be Highly expressed in CSCs. Statins are inhibitors of HMG-CoA reductase, and can reduce CSCs number[81]. Metformin treatment, a known AMPK activator and HMG-CoA reductase inhibitor, can reduce the number of CSCs in prostate cancer. The mevalonate pathway accelerates proliferation in pancreatic cancer CSCs, and atorvastatin can inhibit this proliferation effect[81].

Overall CSCs display notable alterations in metabolic pathways involving a plethora of different substrates, even when compared to normal cancer cells. Targeting metabolism has been demonstrated as a promising way to integrate conventional chemotherapy to unveil vulnerabilities in CSCs. However, given that metabolism has been shown to be strictly controlled by circadian rhythms, it is likely that a deregulation of the intricate interplay between bioenergetic pathways and the clockwork machinery can be an advantageous hallmark for CSCs to evade.

1.5 Cancer stem cells and clock: unexplored territory

The relationship between the clock and stemness is an emerging field of research that carries multiple implications, such as the role of the clock in stemness maintenance and differentiation. Pluripotent stem cells like Embryonic stem cells (ESCs) and induced pluripotent stem cells (iPSCs) typically do not have rhythmic oscillations in clock genes expression, which then arise during differentiation[2]. The same concept seems to be true in the opposite direction: when terminally differentiated cells are reprogrammed to iPSCs using Yamanaka factors (*Oct3/4*, *Sox2*, *Klf4*, and *c-Myc*) circadian oscillatory phenomena are lost[2]. The deregulation of circadian clockwork in stem cells seems to be governed by DNA methyltransferase (*Dnmt1*), found to be essential for both circadian development and differentiation of mouse ESCs[90]. In similar fashion, human ESCs display an induction of *Per2*

rhythmic expression during differentiation into cardiomyocytes, while clock function appeared upon iPSCs differentiation into chondrocytes[2]. It has to be noted anyway that, despite the lack of oscillatory phenomena, clock genes are still expressed in stem cells, suggesting a possible non-canonical role of these genes in stemness maintenance[2,91].

The increasing evidence circadian clock regulation of cancer hallmarks and tumorigenesis is leading scientists to study its role in CSCs, with the hope to specifically target the stem subpopulation in tumors. As of today anyway, studies addressing the circadian rhythm function in CSCs are scares. Arpan De et al. have induced EMT in C6 glioma cells and MCF-7 breast cancer cell *in vitro*, finding enhanced Per2 rhythmic expression and overall circadian gene expression[92]. The stem cell population in this model also showed enrichment in stemness markers (CD133, OCT4) and metastasis markers (ZEB1 and TWIST). Molecular clock synchronization also led to the increase in EMT events 3 hours post synchronization, leading to the speculation that invasion could be more likely to occur at specific circadian times[92].

The relationship linking circadian clock and its role in the regulation of cell proliferation is one of the main focus in cancer pathophysiology. Genetic silencing of BMAL1 or CLOCK can increase cell proliferation in hematological, colon, pancreatic, breast and lung cancer, while overexpression works in the opposite direction, promoting cell cycle arrest and apoptosis[22]. There are evidences that the suppression of proliferation exerted by the clock acts via PER1/2-mediated inhibition of the PI3K/AKT/mTOR signaling cascade[22]. However these study were carried out analyzing the bulk of the tumor rather than CSCs subpopulation, on which studies are needed to clarify the relationship of Clock genes and enhanced proliferative potential[22].

Matsunaga et al. characterized CSCs from mouse 4T1 mammary tumours using ALDH activity as a marker, unveiling how ALDH-positive (ALDH+) cells lacked circadian rhythmic expression of Core clock genes such as *Clock, Bmal1, Per2, Cry1* and *Rev-Erbα*[93]. In contrast, ALDH- cells

displayed robust oscillations of the same genes, suggesting a similar deregulation in CSCs previously observed in ESCs and iPSCs. A follow-up study from the same group revealed that the expression of CLOCK is able to reduce the ALDH+/ALDH- ratio, suppressing stemness and tumor growth[94].

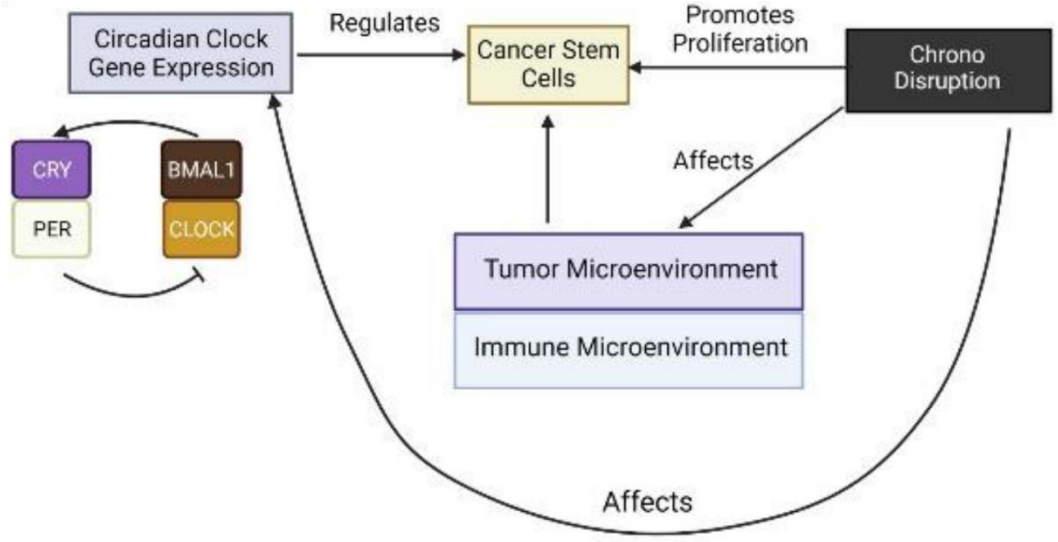

Figure 8. Proposed model on the role of chrono disruption on CSCs proliferation and pasticity[22].

However contrasting evidences are the ones found by Dong et al., as they observed that BMAL1/CLOCK knockdown reduced proliferation and self-renewal in glioblastoma CSCs[95]. In the same study the use of a Rev-Erb agonist was able to downregulate stemness and CSCs growth.

It has been previously observed how circulating tumor cells are regulated in a circadian manner, and that the metastasis burden can be amplified by circadian disruption in MMTW:PyMT mouse model[2]. To date there are no studies that demonstrate direct evidence of circadian rhythms regulating CSCs metastatic potential.

1.5.1 Chronotherapy as a possible anti-cancer treatment

As previously discussed, there is a bulk of evidences pointing toward chronobiology as a key aspect in CSCs biology, thus understanding circadian mechanisms is a matter of particular interest in cancer research.

In the past ten years the timing of chemotherapy administration has been explored as a way to match the patient's circadian rhythms[2]. Given that, depending on the cancer type, some subset of CSCs display active rhythms, a timed administration of drugs could be an effective strategy against those subsets. Conversely, in the case of clock-deficient CSCs, where clock repression may have a pivotal role in self-renewal, stemness maintenance and chemotherapy resistance, thus a possible chronotherapeutic intervention could foresee the pharmacological induction of Core clock genes using Rev-Erb agonists or CRY stabilizers, although there is still a lack of mechanistic understanding on the role of those clock genes in oncogenesis[2].

These potential application are, however, still far from being applicable in a clinical setting, and a deep characterization of molecular mechanism interactions between the clock and Cancer stem cell is needed in order to make chronotherapy a reality in the future.

2 AIMS

The following work stems from the existing literature gap regarding the relationship between Cancer stem cells phenotype and circadian rhythms, with metabolic rewiring and drug resistance being a possible intersection connecting the two.

The first main aim was to perform a circadian phenotypic characterization among several *in vitro* models of Differentiated and Cancer Stem-like cells in order to better understand the still controversial role of clock function in CSC biology.

The second aim was to investigate whether different clock functional profile can influence the circadian regulation of cellular bioenergetics and metabolism.

The third aim was to elucidate the role of circadian rhythms in the enhanced cell proliferation displayed by CSCs, and possibly how clockwork function influences the known drug resistance of CSCs, in the sake to identify new chronotherapeutic targets to adjuvate with conventional chemotherapy.

3 MATERIAL AND METHODS

3.1 Cell cultures

All cell lines used in the present study were purchased from American Type Culture Collection (ATCC, Manassas, VA, USA), except for 3AB-OS cells, which were gently provided by Prof. Luigi Del Vecchio (Department of Molecular Medicine and Medical Biotechnologies, University of Naples Federico II). All cells were cultured at 37 °C in a 5% CO_2 humidified atmosphere in complete DMEM High Glucose medium (25 mM glucose), supplemented with 10% fetal bovine serum, penicillin–streptomycin (100 U/mL) and 2 mM L-glutamine (all these products were purchased from Biowest, Nuaillé, France).

3.2 Synchronization of cultured cells

Clock genes synchronization of cultured cells was performed as previously described in literature[96,97].

Briefly, synchronization was obtained by incubating cells with complete medium supplemented with 0.1 uM dexamethasone for 1 hour; cells were then washed with PBS and the fresh medium was added to allow the cells to settle. Cells were then harvested at different timepoints as indicated in figures.

Serum shock was also used as a synchronization method: cells were incubated for 2 hour in a serum-rich medium (50% FBS), then normal media was then reintroduced.

Cell cultures were typically assayed at a confluence of 80–90%.

3.3 Lentiviral particles production

HEK293T cells were seeded in a T75 flask the day before. For transfection, a total of 600 µL of 2×HBS (CallPhos™ Kit, BD Biosciences #631312) was prepared, containing 8.4 µg of the transfer plasmid (pBMAL-Luc), 6 µg of the packaging plasmid (pPAX), 3.6 µg of the envelope plasmid

(pMD2.G), 526 µL of H_2O (CallPhos™ Kit, BD Biosciences #631312), and 74 µL of the supplied 2 M calcium solution (CallPhos™ Kit, BD Biosciences #631312). The transfection mix was incubated at room temperature for 20 minutes to allow formation of the calcium–DNA complex. Subsequently, 1.75 mL of this mixture was added to the T75 flask containing the HEK293T cells. The culture was incubated overnight in a humidified incubator at 37°C with 5% CO_2. The following morning, a medium change was performed. After an additional 24 hours, the supernatant containing lentiviral particles was collected and stored at 4°C, while fresh medium was again added to the flask. A second harvest of the viral supernatant was performed the next day.

For virus concentration, 1 volume of PEG (polyethylene glycol; Abcam ab102538, PEG Virus Precipitation Kit) was added to every 4 volumes of combined supernatant. The mixture was stored at 4°C for up to 48 hours and then centrifuged at 1,500 × g for 30 minutes at 4°C. The resulting supernatant was centrifuged once more under the same conditions. The two viral pellets were resuspended in cold sterile PBS at 1/100 of the original volume. The concentrated lentiviral stocks were then aliquoted and stored at −80°C until use.

3.4 Lentiviral transduction

Cells were seeded in 6-well plate at 70-90% confluency. For lentiviral infection, cells were incubated for 24 h with media containing 4ug/ul of Polybrene transfection reagent and 5 ul/ml of lentiviral particles.

To ensure the maintenance of stable clones, puromycin was added to the culture media as a selection agent.

3.5 Real-time bioluminescence measurement

The day before the experiment, transduced cells containing the luciferase gene controlled by the BMAL1 promoter were seeded in 35mm dish (Thermo Scientific). Cells were synchronized using 0.1 uM dexamethasone, washed twice with PBS, then DMEM without phenol red and with 250 uM D-luciferin was added. Luciferase activity was measured

by adopting the LumiCycle system (Actimetrics), which allows the real time luminescence measurement in temperature and CO2 controlled conditions. The analysis was carried out using the LumiCycle software: the mean baseline was subtracted from raw luminescence data, which were further analysed with the Cosinor equation. Parameters of the best fitting curves were then statistically analyzed to compare the different cell line oscillations.

3.6 Measurement of proliferation with xCELLigence platform

The xCELLigence System Real-Time Cell Analyzer (ACEA Biosciences, San Diego, CA, USA) was used for monitoring cell proliferation. Cells were seeded at a cell density 4000 cells/well in 16-well E-plates, which was then connected to the RTCA platform placed into a cell incubator at 37 °C and 5% CO2. Approximately 24 h after seeding, medium was removed and cells were synchronized with either serum shock or by media change. Cell proliferation was monitored every 30 min for a period of up to 96 h, measuring changes of electrical impedance as a dimensionless parameter termed cell index (CI). CI was normalized just before treatment and converted into normalized cell index (NCI), calculated as follows: $NCI = CI_{end\ of\ treatment}/CI_{normalization\ time}$, by the RTCA-integrated software (Version 2.0, ACEA Biosciences, San Diego, CA, USA) as previously described[98].

To measure changes in cell proliferation rate, time-resolved measurement of the growth curve slope were plotted by the RTCA-software and subsequently analyzed using the Cosinor equation.

3.7 Reverse Transcriptase Real-time PCR

Total RNA was extracted by using the TRIzol Reagent (#15596026, Invitrogen, Carlsbad, CA, USA) following manufacturer instructions. RNA samples were treated with DNaseI (#18047019, Invitrogen, Carlsbad, CA)

and quantified using Nanodrop ND-1000 (Thermo Scientific, Waltham, MA, USA). 1 ug of RNA was reverse-transcribed using the iScript cDNA Synthesis kit (Bio-Rad Laboratories, Hercules, California, USA).

qPCR was performed using the SsoAdvanced Universal SYBR Green Supermix (#1725271, Bio-Rad Laboratories, Hercules, California, USA) in a CFX96 Touch Real-Time PCR Detection System (Bio-Rad Laboratories, Hercules, California, USA), with each 10 ul reaction containing 50 ng of cDNA as a template. The following primers from Bio-Rad Laboratories (Hercules, California, USA) were used: ARNTL1 (qHsaCID0023313), NR1D1 (qHsaCIP0030036), PER1 (qHsaCID0014451), PER2 (qHsaCID0010055), PER3 (qHsaCEP0049383), CRY1 (qHsaCID0014000) and TBP (qHsaCID0007122). A technical duplicate was performed for each sample. The relative expression of the target genes was quantified using the comparative threshold cycle ($2^{-\Delta\Delta Ct}$) method and normalized to *TBP* levels.

3.8 Western blot

Cells were detached using trypsin 1x (Biowest, Nuaillé, France) and centrifuged at 300 g for 5 minutes. The cell pellet was resuspended in RIPA buffer 1x containing protease and phosphatase inhibitor cocktail (Sigma-Aldrich, St. Louis, MO, USA), and incubated at +4° C for 30 minutes. Cell lysates were then centrifuged at 12.000 g for 15 minutes at +4° C. The supernatant was collected and quantified by Bradford protein assay (Bio-Rad Laboratories, Hercules, CA, USA).

Aliquots of cell lysates, containing 20 µg of proteins, were subjected to SDS polyacrylamide gel electrophoresis using the TGX Stain-Free™ FastCast™ gels (Bio-Rad Laboratories, Hercules, CA, USA) and were subsequently blotted on a nitrocellulose membrane using the Trans Blot Turbo Transfer System (Bio-Rad Laboratories, Hercules, CA, USA) and blocked in a TPBS 1x+ 5% BSA for 1 hour at room temperature or with EveryBlot Blocking Buffer (Bio-Rad Laboratories, Hercules, CA, USA) for 5 minutes at room temperature. Membranes were probed overnight at +4° with the following primary antibodies diluted in TPBS 1x+ 5% BSA: Anti-

Bmal1 (D2L7G) Rabbit mAb, #14020 (1:1000, Cell Signaling Technologies, Danvers, MA, USA), Anti-Rev-Erbα/NR1D1 Rabbit pAb (A18602, ABclonal, Woburn, Massachusetts, US), Anti-β-actin, #A5441 (1:10.000; Sigma Aldrich, St. Louis, MO, USA). Membranes were probed with a correspondingly suited horseradish peroxidase-conjugated secondary antibody (1:5000 for anti-rabbit, 1:3000 for anti-mouse, Bio-Rad Laboratories, Hercules, CA, USA) for 1 hour at room temperature. Chemiluminescent signals were developed using the Clarity Western ECL Substrate (Bio-Rad Laboratories, Hercules, CA, USA), acquired with the ChemiDoc Imager system (Bio-Rad Laboratories, Hercules, CA, USA) and densitometric analysis was performed with the Image Lab 6.1 software (Bio-Rad Laboratories, Hercules, CA, USA).

3.9 Real-time oxygen consumption rate measurement with Resipher® technology

The real time OCR measurement was obtained using the Resipher® platform (Lucid Scientific). 3000 cells/well for 3AB-OS and 5000 cells/well for MG-63 cells were seeded in a 96 multi-well. Assay media was allowed to equilibrate in the cell incubator at 37° C, 5% CO2 overnight. After synchronization with 0.1 uM dexamethasone, the assay media was added to each well to a final volume of 200 ul. The respiratory profile was monitored through the https://lab.lucidsci.com portal. At the end of the experiment, the mean baseline values was subtracted from the raw OCR values to obtain the first derivative or the slope rate-of-change of the curve which was then analysed with the Cosinor equation.

3.10 Metabolic flux analysis

Metabolic flux analysis was performed using an XF96 extracellular flux analyzer (Agilent Technologies, Santa Clara, CA, USA), which allows for the simultaneous measurement of Oxygen consumption rate (OCR) and Extracellular acidification rate (ECAR). Briefly, cells were seeded onto a

Seahorse 96-well plate at a density of 4000 cells/well for MG-63 and 5000 cells/well for 3ABOS cells and were allowed to settle overnight. To allow for a common end-point measurement for different time points, cells were subjected to a modified synchronization protocol following a 4-h out-of-phase time-schedule. The day of the assay, the growth medium was replaced with 180 µL of bicarbonate-free DMEM supplemented with 25 mM glucose, 2 mM glutamine and 1 mM sodium pyruvate (all purchased from Sigma-Aldrich, St. Louis, MO, USA) . Cells were preincubated in a CO_2-free incubator at 37 °C for 45 minutes.

OCR was measured under basal conditions and after sequential injection of oligomycin (1 µM), carbonyl cyanide-p-trifluoromethoxyphenylhydrazone, FCCP (0,5 µM), and rotenone + antimycin A (1 µM + 1 µM) to evaluate the ATP-linked respiration, the maximal respiratory capacity, and the non-mitochondrial oxygen consumption, respectively. For ECAR analysis 50 mM 2-deoxyglucose was added in order to determine the glycolysis-independent acidification. The OCR and ECAR values were normalized to the protein content in each well, quantified by BCA assay (Thermo Scientific, Waltham, MA, USA).

The cellular ATP production rates were quantified using the Agilent Seahorse XF ATP real-time assay kit using label-free technology in real time as specified by the manufacturer. Briefly, glycolytic ATP production rate can be derived stoichiometrically from the glycolytic acidification measurement (glycolytic proton efflux rate, glycoPER) according to the following equation:

glucose + 2 ADP +2 Pi → 2 lactate + 2 ATP + 2 H2O + 2 H^+;

the glycolytic proton efflux rate (glyco PER) was determined by accounting for the medium buffering factor (BF). BF was calculated separately by measuring pH changes elicited by consecutive additions of titrated HCl in 5 mM Hepes-supplemented DMEM. The mitochondrial ATP production rate (mitoATP) was equal to OCR_{ATP} x 2 x P/O (mol ATP/mol O), where OCR_{ATP} was the difference between the basal OCR and the OCR in the presence of

oligomycin; a theoretical P/O ratio of 2.75 was assumed based on the combined oxidation of glucose, fatty acid, and glutamine.

3.11 Polar metabolites and lipids extraction

Cellular pellets were resuspended with 500µL of cold methanol (MeOH), vortexed and incubated on ice for 20 minutes to extract polar metabolites. Then, samples were vortexed and centrifuge at 800 g for 1minute a 0°. Supernatant was collected, while the pellet was subjected to two additional extraction steps, first with 500 µL of MeOH, then with 250µL of MilliQ water (H2O), both followed by vortex and centrifugation. At each step supernatant was recovered. Finally, the combined supernatants were split to analyze separately polar metabolites and lipids, dried, and finally reconstituted as follows: 80 µL of acetonitrile (ACN) and H2O (50:50 v/v) for polar metabolites analysis, 80 µL of isopropanol (ISO) for lipids analysis. Quality control samples (QC samples) were prepared pooling 10 µL of each sample in a single tube.

3.12 LC-MS analysis

Samples were analyzed using an UHPLC-MS platform which includes an Agilent 1290 II liquid chromatography system coupled to a quadrupole-time-of-flight mass spectrometer (Q-TOF – Agilent Technologies, Palo Alto, CA, USA). The chromatographic separation for polar analytes was achieved using an InfinityLab Poroshell 120 HILIC-Z (2.1 x 150mm 2.7µm) column, the chromatographic eluents were: A, 100% 20mM ammonium acetate and 5µM medronic acid; B, 100% ACN. The gradient applied was: 0 min 90%B, 1 min 90%B, 8 min 78%B, 12min 60%B, 15 min 10%B, 18 min 10%B, 23 min 90%B, at flow rate of 0.4 mL/min. The mass spectrometer operates at a resolution of 40000 FWHM with a full scan range of 40-1200 m/z in both positive and negative polarity. On the other hand, the lipidome separation was achieved with ACQUITY UPLC CSH C18 Column (2.1 x 100 mm, 1.7µm - Waters, Milford, MA, USA). The mobile phases for chromatographic separation were: A, 10 mM ammonium

acetate:ACN 40:60 v:v with 0.1% acetic acid; B, ISO:phase A 90:10 v:v. The elution gradient was: 0 min 99% A, 1 min 99% A, 1.10 min 60% A, 5 min 20% A, 11 min 20% A, 12 min 1% A, 18 min 1% A, 18.10 min 60% A, 20 min 99% A, at flow rate of 0.25 mL/min. The resolution of the mass spectrometer was set at 50000 FWHM and it operates in full scan range of m/z 100-1350. The samples were analyzed in full scan mode in triplicate both in positive and negative ESI mode. QCs were used to monitor the performance of the analysis and were injected every 5 samples. At the end of the analysis, 5 injections of QCs were used to collect MS/MS spectra in data dependent mode (DDA) using an iterative approach.

3.13 Metabolomics data analysis and statistics

Mass Profiler Professional Software provides a comprehensive platform for processing and analyzing data obtained from Agilent mass spectrometers and was used for raw data analyses. The tool MassHunter Profinder permits a rapid batch-processing feature integration and annotation using LC/MS Personal Compound Databases. Our in-house library for polar metabolites and lipids was built based on accurate mass, MS/MS, isotopic pattern and retention time, and using online databases as HMDB [REF: 10.1093/nar/gkx1089] and METLIN [REF: 10.1021/acs.analchem.7b04424]. The samples analyzed in Full scan were matched based on mass formula extraction and retention time against our in-house database.

The extracted data were normalized by the sum of the intensity of all the features, and then log10 transformed and mean centered before univariate and multivariate analyses using Metaboanalyst 6.0 [REF: 10.1093/nar/gkae253]. Exploratory Principal Component Analysis (PCA) was applied to detect specific patterns in the data. Student's t-Test with False Discovery Rate (FDR) was performed to complete the results of multivariate data analysis. Variables with FDR p-values less than 0.05 were selected as significant data. Enrichment pathway analysis was performed on the relevant identified metabolites and lipids using enrichment analysis tool

on Metaboanalyst 6.0 and with LION/web [REF: 10.1093/gigascience/giz061], respectively.

3.14 COSINOR Analysis

Time-resolved data points were subjected to non-linear regression analysis by using the Cosinor equation[99]:

$$f(t) = M + A \cdot e^{(t \cdot a)} \cdot \cos\left(2\pi \cdot \frac{t - \varphi}{P}\right) + s \cdot t$$

where the following parameters were obtained: M = *MESOR* (Midline Statistic Of Rhythm, a rhythm-adjusted mean), A = amplitude (a measure of half the extent of predictable variation within a cycle); P = period (duration of one cycle); and ϕ = acrophase (a measure of the time of overall high values recurring in each cycle, corresponding to the time post-synchronization when the first peak appears). The parameters of the best-fitting curve were then subjected to statistical analysis. The non-linear fit was performed using the *GraFit* software (V 4.0.13, Erithacus Software Limited, East Grinstead, West Sussex, UK).

3.15 Statistical analysis

Data are presented as mean±SEM or mean±SD. Data were analysed with Welch's t-test or one or two-way ANOVA followed by Sidak's post-hoc test for multiple comparisons. p-values<0,05 were considered as statistically significant. All statistical analysis were performed using *Graph Pad Prism* (Graph Pad software, v 10.6, San Diego, CA, USA).

4 RESULTS AND DISCUSSION

4.1 CSCs display an overall deregulation of Bmal1 promoter function

In order to evaluate the circadian function in Differentiated Cancer cells (DCCs) and CSCs, we choose several models of bladder cancer, breast cancer and osteosarcoma, and for each one we selected a differentiated and a stem-like cell line, having in this way *in vitro* models that recapitulate the tumor bulk-CSCs dichotomy. In the bladder cancer model we choose RT4 cell line as a DCCs, as it derives from a non-invasive, well differentiated transitional cell papilloma[100]; the CSCs counterpart we selected is the T24 cell line, a muscle-invasive form of bladder cancer, which also express EMT and stem cell-like markers such as CD44 [101–103]. The osteosarcoma model saw the use of differentiated cells, MG-63, and cancer stem cell line 3AB-OS, which was obtained from long-term exposure of MG-63 to 3-aminobenzamide, resulting in the selection of a CD133+ stem sub-clone of the original cell line[104]. In the case of breast cancer, we adopted the MCF-7 cell line, expressing estrogen, progesterone and androgen receptor, resembling differentiated, hormone responsive, non-aggressive breast cancer[105,106], and MDA-MB-231 cells, a highly aggressive, triple negative breast cancer cell line, which also express the stemness marker CD44[107,108].

We performed lentiviral transduction to obtain stable clones of each cell line, expressing a sequence bearing the luciferase gene preceded by the Bmal1 promoter. In this way the expression of the luciferase under control of the Bmal1 promoter activity can serve as a proxy measurement of the circadian machinery functionality at the molecular level[109]. Analysis of real-time bioluminescence following clock synchronization in the bladder cancer model revealed a robust rhythmic oscillation in Bmal1 promoter activation in RT4, characterized by a 20 hour period (Figure 9 A). On the other hand, T24 stem-like cells displayed a quite dampened profile, as the amplitude of the curve was significantly reduced, while the period did not change (Figure

9 A). The first positive peak (acrophase) in Bmal1 promoter activity was also shifted ahead in T24 (Figure 9 A).

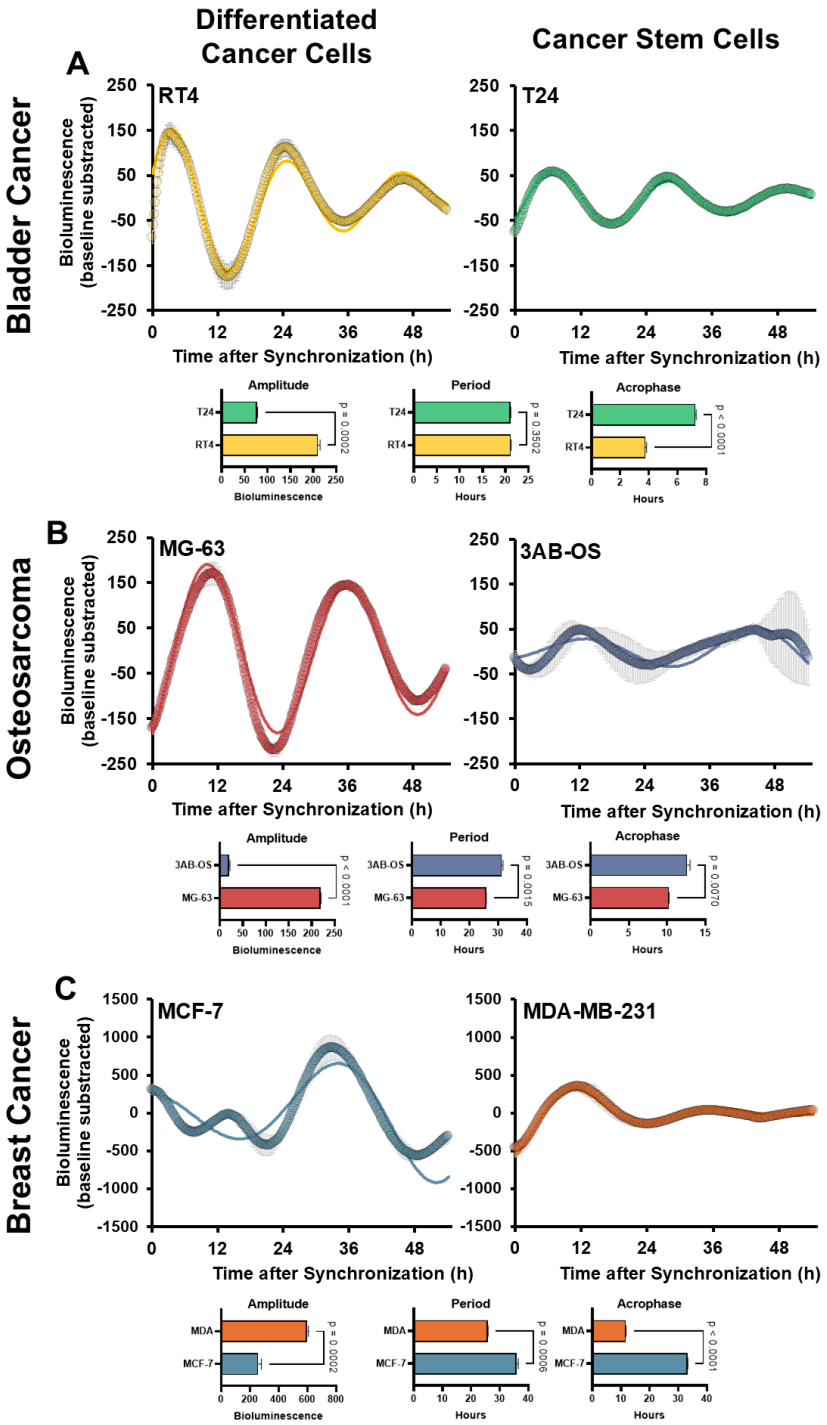

Figure 9. Real time bioluminescence monitoring of pBMAL1::luc transfected cells. Bladder (A), osteosarcoma (B) and breast (C) cancer cells lentivirally transduced with pBMAL1::luc construct were synchronized and bioluminescence was measured over 48 hours. Round dots represent mean±SEM of N=3 independent experiments; continuous line represents Cosinor best fit values. Histograms represents Cosinor fitting values (mean±SD), which were compared using Welch's t-test, p value are shown for each comparison.

Similarly to what we found in RT4, in differentiated osteosarcoma cells MG-63 Bmal1 promoter activation followed a very robust, 24 hour circadian profile (Figure 9 B), while in 3AB-OS stem sub-clone the amplitude was dramatically reduced in a significant way, as well as a longer oscillatory period and higher acrophase, suggesting an overall deregulation of circadian function in osteosarcoma CSCs.

In breast cancer we observed in MCF-7 differentiated cells that Bmal1 promoter undergoes a strong activation 24 hours after synchronization (Figure 9 C), with a peak at about 36 hours post dexamethasone treatment, while in other DCCs the acrophase was at about 10-12 hours post synchronization. In MDA stem-like cells we observed a completely reversed phenotype, with a quick response and then a rapid loss of the synchronization stimulus in the Bmal1 promoter activity (Figure 9 C).

These findings indicate that DCCs display quite strong rhythmicity in the Bmal1 promoter activity, thus suggesting a functional molecular clockwork, although the oscillatory profile tended to vary when taking into considerations different tumor types. In CSCs we found an opposite phenotype, where the rhythmic activation of the molecular clock had a less marked amplitude, with a strong attenuation of the oscillation as time progressed, resulting in an overall less robust pattern, which could be an indication of poor circadian function.

4.2 mRNA expression and circadian pattern is impaired in CSCs

Stemming from the previously shown results, we then focused our attention on the osteosarcoma model for two reasons: being 3AB-OS a direct sub-clone derived from the differentiated counterpart, this model is the only one recapitulating with higher fidelity the tumor bulk-CSCs dichotomy, thus it is an ideal model to study intratumoral heterogeneity; secondly, this model has been extensively characterized in the past both from a molecular and metabolic plasticity point of view and also regarding chemoresistance[104,110,111], making it the most relevant model to the aims of

the project.

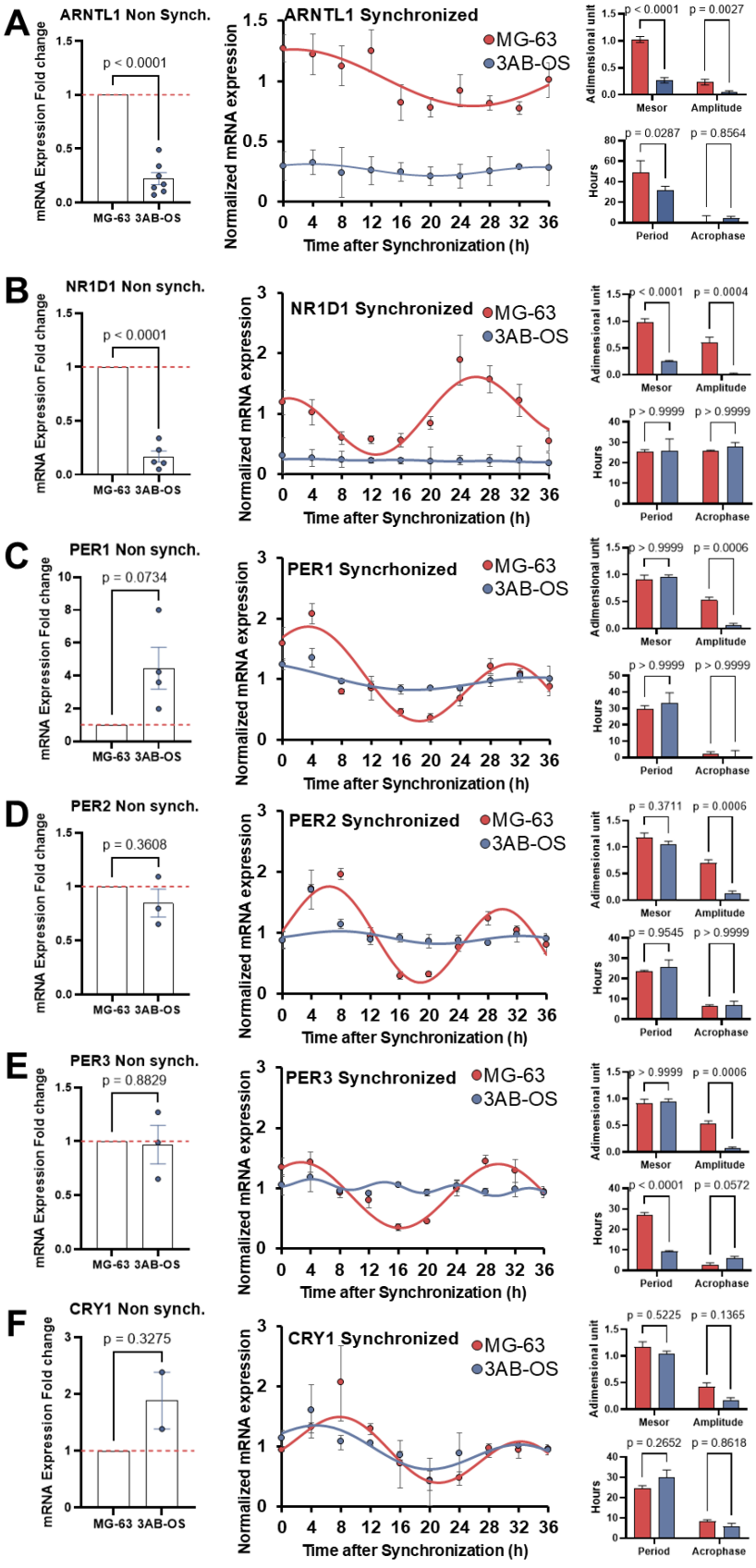
A
ARNTL1 Non Synch.
mRNA Expression Fold change
p < 0.0001
MG-63 3AB-OS
ARNTL1 Synchronized
MG-63
3AB-OS
Normalized mRNA expression
Time after Synchronization (h)
Adimensional unit
p < 0.0001
p = 0.0027
Mesor
Amplitude
Hours
p = 0.0287
p = 0.8564
Period
Acrophase
B
NR1D1 Non synch.
p < 0.0001
NR1D1 Synchronized
p < 0.0001
p = 0.0004
p > 0.9999
p > 0.9999
C
PER1 Non synch.
p = 0.0734
PER1 Syncrhonized
p > 0.9999
p = 0.0006
p > 0.9999
p > 0.9999
D
PER2 Non synch.
p = 0.3608
PER2 Synchronized
p = 0.3711
p = 0.0006
p = 0.9545
p > 0.9999
E
PER3 Non synch.
p = 0.8829
PER3 Synchronized
p > 0.9999
p = 0.0006
p < 0.0001
p = 0.0572
F
CRY1 Non synch.
p = 0.3275
CRY1 Synchronized
p = 0.5225
p = 0.1365
p = 0.2652
p = 0.8618

Figure 10. Core clock genes expression in osteosarcoma differentiated and stem cancer cells. mRNA expression levels of ARNTL1 (A), NR1D1 (B), PER1 (C), PER2 (D), PER3 (E) and CRY1 (F) measured with qPCR. In non-synchronized conditions bar graphs represent mRNA expression normalized to TBP levels relative to MG-63, shown as mean±SEM, where dots represent each biological replicate. In synchronized experiments, plotted round dots represent mRNA expression normalized to TBP relative to MG-63 average, shown as mean±SEM of N=3 independent biological replicates values; continuous line represents Cosinor best fit values. Bar graphs on the right represent Cosinor fitting parameters (mean±SD); two-way ANOVA with Sidak's post hoc test for multiple comparisons was used to compare Cosinor fitting values; p-values are shown for each comparison.

We therefore proceeded to perform a molecular characterization of the circadian phenotype of the osteosarcoma model, finding that basal level of the master clock regulator *ARNTL1* (the gene encoding for Bmal1 protein) and secondary feedback loop member *NR1D1* (the gene econding for Rev-Erbα) transcript was strongly reduced in 3AB-OS (Figure 10 A-B). We also measured *PERs* and *CRY1* mRNA expression, finding only in PER1 a non-significant increase in CSCs (Figure 10 C-F). We then measured mRNA expression in synchronized cells, revealing a similar scenario previously observed, where 3AB-OS have an altered oscillatory patter in *ARNTL1* (Figure 10 A) compared to MG-63, showing a significant reduction in mesor, amplitude and period. The results were even more dramatic when examining *NR1D1* oscillatory patter, which in MG-63 followed a robust 24 hours circadian profile, whereas in CSCs was completely abolished, as the mesor and amplitude were significantly lower (Figure 10 B). A similar outline could be drawn when taking into account *PER1/2/3*, where the rhythmic profile in CSCs is absent even if the basal gene expression is not changing compared to MG-63 (Figure 10 C-E), suggesting a potential non canonical role of *PER* genes in 3AB-OS. In *CRY1* oscillatory expression we found no significant differences between the two cell lines (Figure 10 F).

Overall the results corroborated the previously obtained data, showing a substantial impairment in the canonical clockwork functionality in osteosarcoma CSCs.

4.3 Differential protein expression pattern in Differentiated and Stem Cancer cells

Next we focused the attention on Bmal1 and Rev-Erbα, being the two CCGs that were substantially deregulated in both the basal mRNA expression level and in the circadian profile in CSCs. Western blotting analysis in non-synchronized cells confirmed the reduced Bmal1 protein expression in 3AB-OS cells (Figure 11 A), which was previously observed in the transcript analysis. However, this was not true in the case of Rev-Erbα, where protein expression levels in basal conditions were upregulated in 3AB-OS (Figure 11 C), whereas the mRNA levels showed an opposite trend. One possible explanation to this counterintuitive result could be that in 3AB-OS Rev-Erbα mRNA levels are low because of low levels of its transcriptional activator, Bmal1, while Rev-Erbα protein accumulates possibly due to slower degradation rate. Previous reports have also shown that the transcription factor c-myc is involved in clock genes regulation: similarly to Bmal1, c-myc contains a basic helix-loop-helix motif, which allows its binding to E-box sequences found in promoter regions; c-myc upregulation in U2OS cells is able to modulate and disrupt the clockwork by inducing Rev-Erbα expression, which then inhibits Bmal1 protein expression[70]. Coherently with this scenario, we observed an upward trend of c-myc expression in 3AB-OS cells, which could explain the Rev-Erbα increase and Bmal1 reduced protein levels when compared to MG-63 cells (Figure 11 B).

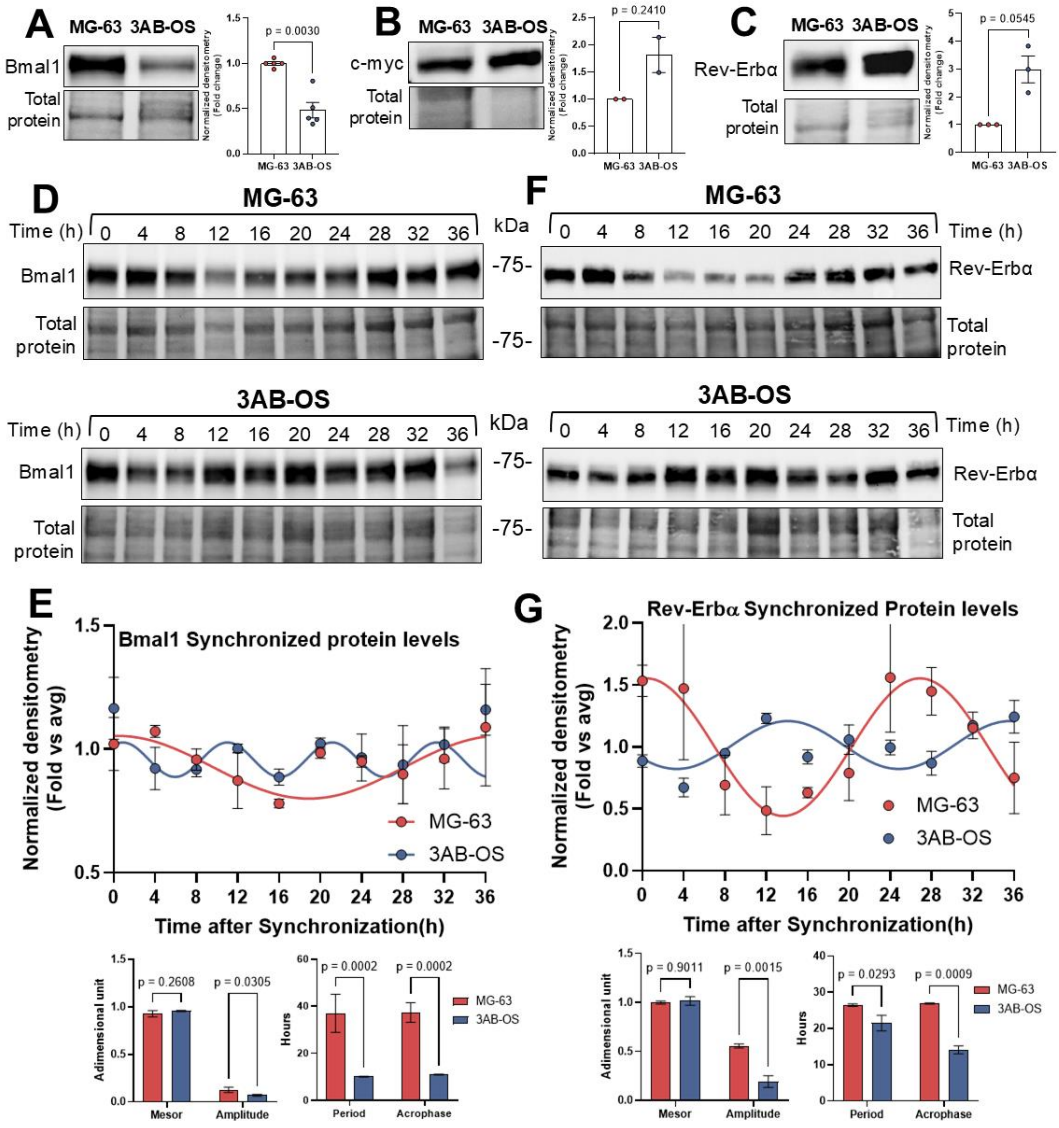

Figure 11. Basal and synchronized protein expression analysis of Bmal1 and Rev-Erbα. Protein expression analysis by means of western blotting. Representative basal level blot and relative densitometry of Bmal1 (A) c-myc (B) and Rev-Erbα (C), bar graphs show the densitometry of the bands normalized to the adjusted total lane protein stain, shown as mean±SEM, where dots indicates each biological replicate; Welch's t-test was performed to compare the groups, p-values are shown.
Representative blots of Bmal1 (D) and Rev-Erbα (F) protein expression in synchronized MG-63 and 3AB-OS cells; Time-resolved densitometric analysis of bands for each time point normalized to the adjusted total lane protein stain for Bmal1 (E) and Rev-Erbα (G), where round dots represent mean±SEM of N=2-3 independent biological replicates values normalized to average of the entire datasets; continuous line represents Cosinor best fit curve; bar graphs represents Cosinor fitting values (mean±SD); two-way ANOVA with Sidak's post hoc test for multiple comparisons was used to compare Cosinor fitting values; p-values are shown for each comparison.

We then switched to synchronized cells, where once again Bmal1 protein expression showed substantial alteration in the oscillation in 3AB-

OS when compared to the differentiated counterpart (Figure 11 D-E), with its amplitude being reduced. The Bmal1 period in CSCs also is significantly reduced (Figure 11 D-E), suggesting that the differences of Bmal1 protein levels over time could be the result of an uncoordinated variation in protein level rather than a regulated oscillation.

In differentiated cells Rev-Erbα protein levels followed a robust and significant circadian pattern (Figure 11 F-G). CSCs in contrast displayed a reduced amplitude and period, as well as shifted acrophase (Figure 11 G-G).

Overall, we were able to characterize the circadian phenotype of osteosarcoma DCCs and CSCs at the molecular level, thus we demonstrated that 3AB-OS stem-subclone display a deregulation in clockwork function.

4.4 Proliferation rate displays an ultradian oscillation profile in Differentiated Cancer cells, but not in Cancer stem cells

Being enhanced proliferation both a known clock-controlled cancer hallmark and a CSCs prominent feature, we next assessed the proliferative potential of osteosarcoma DCCs and CSCs. It well recognised the antithetic role of Bmal1 and Rev-Erbα on the regulation of cell cycle and proliferation, as the circadian master regulator is an inhibitor of cell proliferation, whereas Rev-Erbα acts as a stimulator of it[61,62]. Given the differential expression of both proteins between 3AB-OS stem cells and MG-63 differentiated cells, we used the xCELLigence platform from Agilent, which allows for real time high-resolution impedentiometric measurement of cell proliferation, to study the impact of the different circadian phenotype of the two cells on proliferation. Firstly we confirmed the higher proliferative potential of 3AB-OS compared to parental MG-63 (Figure 12 A-B)[104]. We then plotted the slope of the growth curve at each time point, obtaining a time-resolved measurement of the proliferation rate, which unveiled that MG-63 differentiated cancer cells display a ultradian (17h period) oscillation in the proliferation rate values (Figure 12 C-D). In contrast CSCs have a complete abolishment of proliferation rate oscillation, having in this

way a higher mesor compared to DCCs, meaning that over time their growth is more pronounced and uncontrolled (Figure 12 C-D).

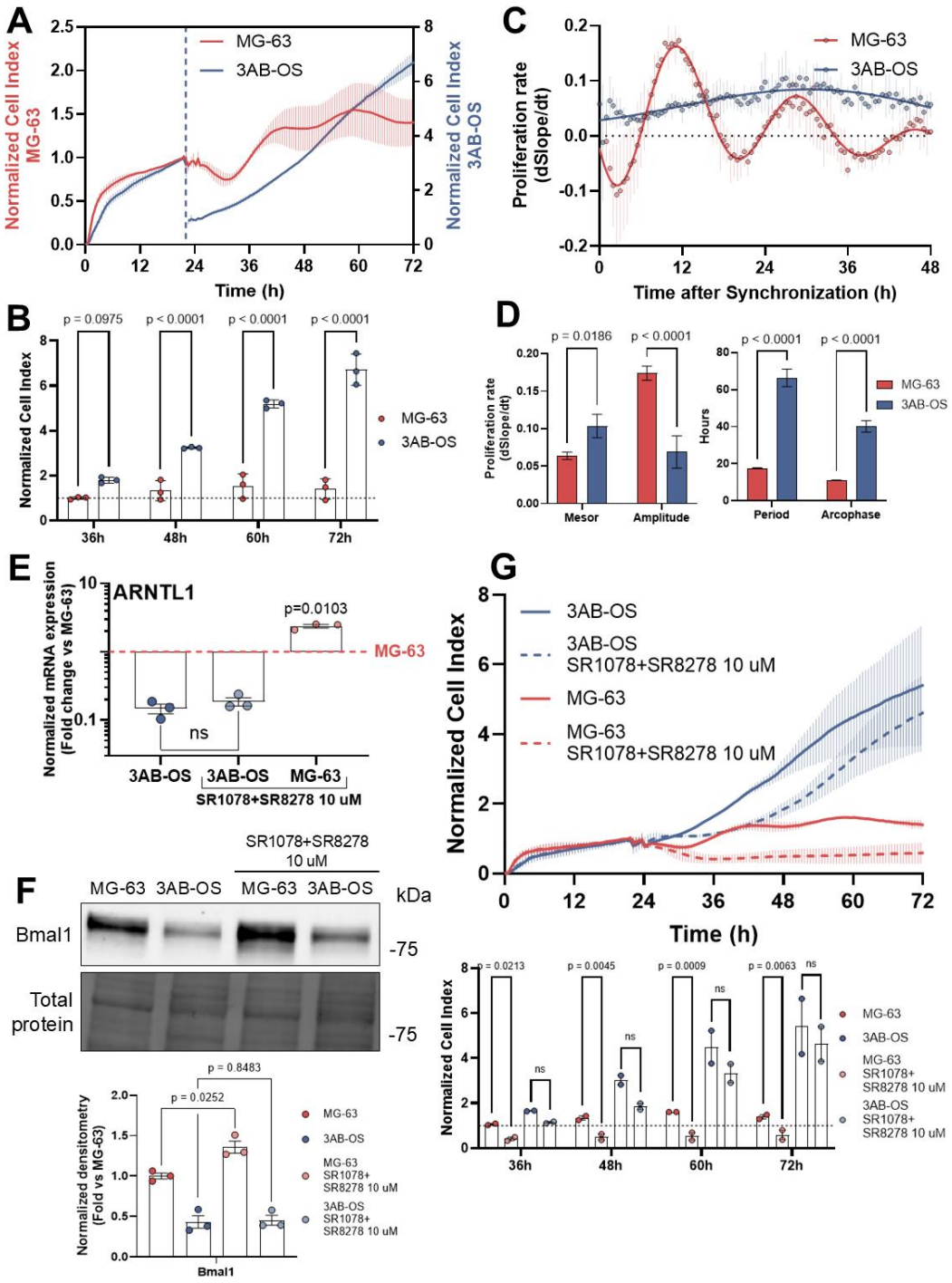

Figure 12. Proliferation assay in DCCs and CSCs. xCELLigence traces (A) of N=3 independent experiments of MG-63 (in red), 3AB-OS (in blue); bar graphs (B) represent Normalized Cell Index at different time points showed as mean±SEM, with each point showing values of each biological replicate (N=3); statistical analysis with two-way ANOVA and Sidak's post hoc test for multiple comparisons was performed, p-values are shown for each comparison.
The slopes of the proliferation curve were plotted of each time point to obtain the time-resolved proliferation rate (C) graphs, where dots represent the mean±SEM of N=3 biological replicates and the continuous line shows the Cosinor best fit curve; Bar graphs (D) show mean±SD of Cosinor fitting parameters, which were then analysed using two-way ANOVA with Sidak's post hoc test for multiple comparisons. p-values are shown.
(E) shows qPCR analysis of ARNTL1 mRNA expression levels normalized to TBP relative to MG-63 following Rev-Erbα antagonist and Rorα agonist pharmacological treatment; the dotted red line represent the MG-63 treated with DMSO as vehicle and bar graphs represent the fold change mean±SEM of N=3 independent biological replicates; statistical analysis was performed with Welch's t-test to compare each treated sample with the untreated control; p-values are shown.
(F) shows representative Bmal1 blot and densitometric analysis of the bands normalized to adjusted total lane protein stain, where bar graphs show mean±SEM of N=3 independent biological replicates, which were then analysed using two-way ANOVA with Sidak's post hoc test for multiple comparisons. p-values are shown. xCELLigence traces (G), where the continuous line represents the controls, dashed line are treated cells and bar graphs represents Normalized Cell Index of N=2 independent experiments; statistical analysis was performed using two-way ANOVA with Sidak's post hoc test for multiple comparisons. p-values are shown.

To our knowledge, this is the first report of a circadian proliferative rate oscillatory profile in osteosarcoma cells, while previous evidences on circadian impact on tumor growth rate have been uncovered in an *in vivo* breast cancer model[112] and *in vitro* on melanoma and colorectal cancer cell lines[113]. Moreover, these are the first observation that the abrogation of clock function in osteosarcoma cancer stem cells is associated to a lack of circadian proliferation rate profile.

4.5 CSCs are refractory to pharmacological clock induction

Since it is reported that clock controls cell proliferation and in our model the proliferation rate reflects the clock-functioning phenotype in DCCs and the clock-lacking phenotype in CSCs, we wondered whether enhancing clock function could serve as an anti-proliferation treatment in tumors. We used a combined treatment consisting of Rev-Erbα antagonist SR8278 and Rorα agonist SR1078, which were chosen as a strategy to induce Bmal1 expression in our model. We revealed a significant 2.3-fold

increase in Bmal1 mRNA expression in DCCs upon combined treatment (Figure 12 E), which was further confirmed in protein expression analysis with a significant increase of the circadian master regulator (Figure 12 F). In CSCs however, we only achieved a modest and non-significant Bmal1 induction after treatment in mRNA levels (Figure 12 E), while protein levels were not affected (Figure 12 F).

Cell proliferation assay showed that Bmal1 induction leads to cell toxicity and inhibition of proliferation in clock-functioning DCCs (Figure 12 G), while 3AB-OS cells were not only refractory to Bmal1 stimulation, but the proliferation was not impacted after SR8278+SR1078 treatment (Figure 12 G). The result obtained suggest that the clock suppression in CSCs confers a refractivity to exogenous circadian stimuli and thus a proliferative advantage to 3AB-OS cells.

4.6 Loss of circadian clock in CSCs confers a flexible metabolic profile

Following the molecular and proliferative circadian characterization, we focused our efforts on another key clock-controlled cancer hallmark, metabolic rewiring. As a first step we performed real-time measurements of oxygen consumption rate (OCR) as a proxy of mitochondrial activity in both cell lines by using the Resipher® platform (Lucid Scientific). The analysis revealed that in MG-63 cells the basal cellular OCR followed a circadian pattern (Figure 13 A-C), with a period of about 24 hours, in accordance with previous observations that demonstrated how the circadian clock dictates mitochondrial function oscillations[46,49,51]. Once again, in contrast to DCCs, 3AB-OS stem sub-clone showed a less robust oscillation, as evidenced by reduced amplitude and higher period compared to MG-63 cells (Figure 13 B-C).

To gain more insight into circadian-related bioenergetic metabolism in osteosarcoma CSCs, we switched to the Seahorse platform in order to obtain a more accurate assessment of mitochondrial function using respiratory chain inhibitors, which confirmed the previous result where

MG-63 cells have a circadian oscillatory profile of mitochondrial respiration (Figure 13 D), while 3AB-OS display an uncontrolled decrease of OCR over time after synchronization (Figure 13 D), while mitochondrial ATP production rate followed a similar pattern in both cell lines (Figure 13 G). The Seahorse methodology also enabled us to measure the extracellular acidification rate (ECAR) as an assessment of the anaerobic glycolytic flux and glycolysis derived ATP production rate, both of which were particularly pronounced in CSCs (Figure 13 E-H), probably to compensate the dropping trend in mitochondrial respiration over time observed previously, while in MG-63 ECAR measurements were relatively stable and much lower (Figure 13 E), in accordance with previous reports on the same cells[110,111]. Altogether the metabolic flux analysis revealed that clock-controlled MG-63 cells tend to have bioenergetic oscillations in a circadian manner, remaining mainly oxidative and clustered over time, as it is evident in the energy map shown in Figure 13 F. Clock-deficient 3AB-OS CSCs on the other hand went from slightly oxidative to energetic, to glycolytic, to quiescent, displaying a less clustered and highly plastic metabolic phenotype throughout the hours after synchronization (Figure 13 F). The ATP production rate map (Figure 13 I) describes a similar pattern[114]: MG-63 in each time point observed after synchronization were grouped above the identity line plotted (which indicates the region of the map where a cell has equal ATP production contribution from Glycolysis and OXPHOS), meaning that they draw more than 50% of ATP production from mitochondria, while, despite having a higher degree of metabolic plasticity, CSCs were positioned mainly in the lower part of the map, meaning that glycolysis is the main pathway from which they satisfy their ATP demand.

The time-resolved metabolic fluxes characterization demonstrated the circadian rhythmicity of mitochondrial respiration in MG-63, which was lost in the clock-deficient stem-subclone 3AB-OS, that once again showed a marked glycolytic-oriented and plastic metabolic phenotype.

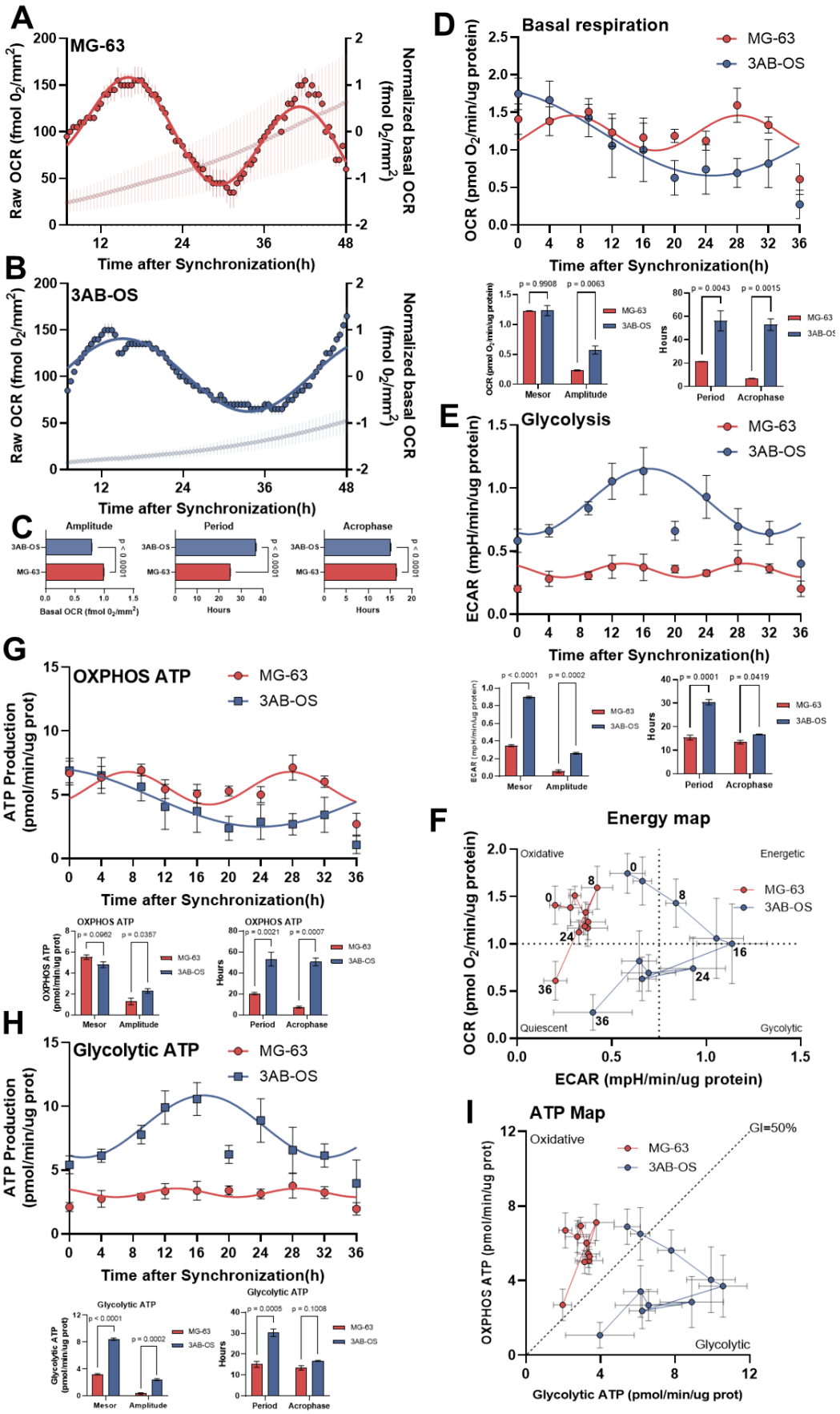
A
MG-63
Raw OCR (fmol O_2/mm^2)
Normalized basal OCR (fmol O_2/mm^2)
Time after Synchronization(h)
B
3AB-OS
C
Amplitude
Period
Acrophase
Basal OCR (fmol O_2/mm^2)
Hours
D
Basal respiration
MG-63
3AB-OS
OCR (pmol O_2/min/ug protein)
Mesor
Amplitude
Period
Acrophase
E
Glycolysis
ECAR (mpH/min/ug protein)
F
Energy map
Oxidative
Energetic
Quiescent
Glycolytic
G
OXPHOS ATP
ATP Production (pmol/min/ug prot)
H
Glycolytic ATP
I
ATP Map
GI=50%
OXPHOS ATP (pmol/min/ug prot)
Glycolytic ATP (pmol/min/ug prot)

Figure 13. Real time respirometric analysis and time point metabolic flux analysis. Real time OCR monitoring in MG-63 (A) and 3AB-OS (B), where dots represents the mean±SEM of OCR measurements, continuous line shows Cosinor fitting of the experimental points; bar graphs (C) represents mean±SD of Cosinor parameters, Welch's t-test was used to perform statistical analysis, p-values for each comparisons are shown. Time-point measurement of Basal respiratory rates (D) and Glycolytic activity (E) in synchronized cells performed using Seahorse platform, where dots represent mean±SEM of N=2 independent experiments of OCR (D), ECAR (E), OXHPOS ATP production (G) and Glycolytic ATP production (H) measurements obtained as specified in materials and methods, continuous line represents Cosinor fitting of experimental points; bar graphs represents Cosinor parameters as mean±SD, which were then compared using two-way ANOVA with Sidak's post hoc test for multiple comparison, p-values are shown for each comparison. Energy map (F) and ATP map (I) obtained by plotting the ECAR and OCR measurements shown in (D) and (E) or Glycolytic ATP and OXPHOS ATP measurements shown in (G) and (H) respectively.

4.7 Glycolytic and TCA cycle metabolites recapitulate the cellular bioenergetic profile

To follow the bioenergetic study, we performed time-resolved untargeted metabolomic analysis of synchronized cells, in particular of polar metabolites belonging to the glycolytic pathway and the TCA cycle. Principal component analysis unveiled a clustered and coordinated changes of metabolites over time in MG-63 cells (Figure 14 B), while 3AB-OS, similarly to what we observed in the bioenergetic map, showed a lower degree of clustering.

To gain more insight from the untargeted analysis, we adopted a series of ratios between the relative abundance of metabolites as proxy measurements for the different metabolic fluxes: the anaerobic glycolysis was assessed measuring the lactate/glucose ratio, which in 3AB-OS stem cells followed a similar pattern observed previously in the glycolytic activity measurement obtained from the Seahorse analysis, with a peak between 16 and 28 hours post-synchronization (Figure 14 C). This result is coherent with previous reports indicating 3AB-OS cells as strongly glucose dependent[110]. In MG-63, similarly to what was found in the metabolic flux analysis, there was a less pronounced oscillation in the Lactate/glucose ratio. The pyruvate/glucose ratio, a proxy measure of aerobic glycolysis, did not follow any substantial pattern (Figure 14 D).

We then used the α-ketoglutarate/glutamine ratio as a measure of glutamine shunting in the TCA cycle, finding that MG-63 cells display circadian peaks in glutamine utilization at 8 and 30 hours post synchronization (Figure 14 E), at the same time points where mitochondrial respiration reaches its maximum values, suggesting that glutamine oxidation is one of the main fuelling pathways used by DCCs. This result is also consistent with existing evidence demonstrating the glutamine-dependency of MG-63 cells[111]. Glutamine and OCR peaks also are coincidental to peaks in ATP/ADP ratio, indicating high intracellular energy balance (Figure 14 H), thus corroborating the suggestion that the major contribution to cellular ATP derives from mitochondrial glutamine oxidation in MG-63 cells. 3AB-OS cells in turn display low utilization of glutamine (Figure 14 E), coherently with the more glycolytic-oriented phenotype.

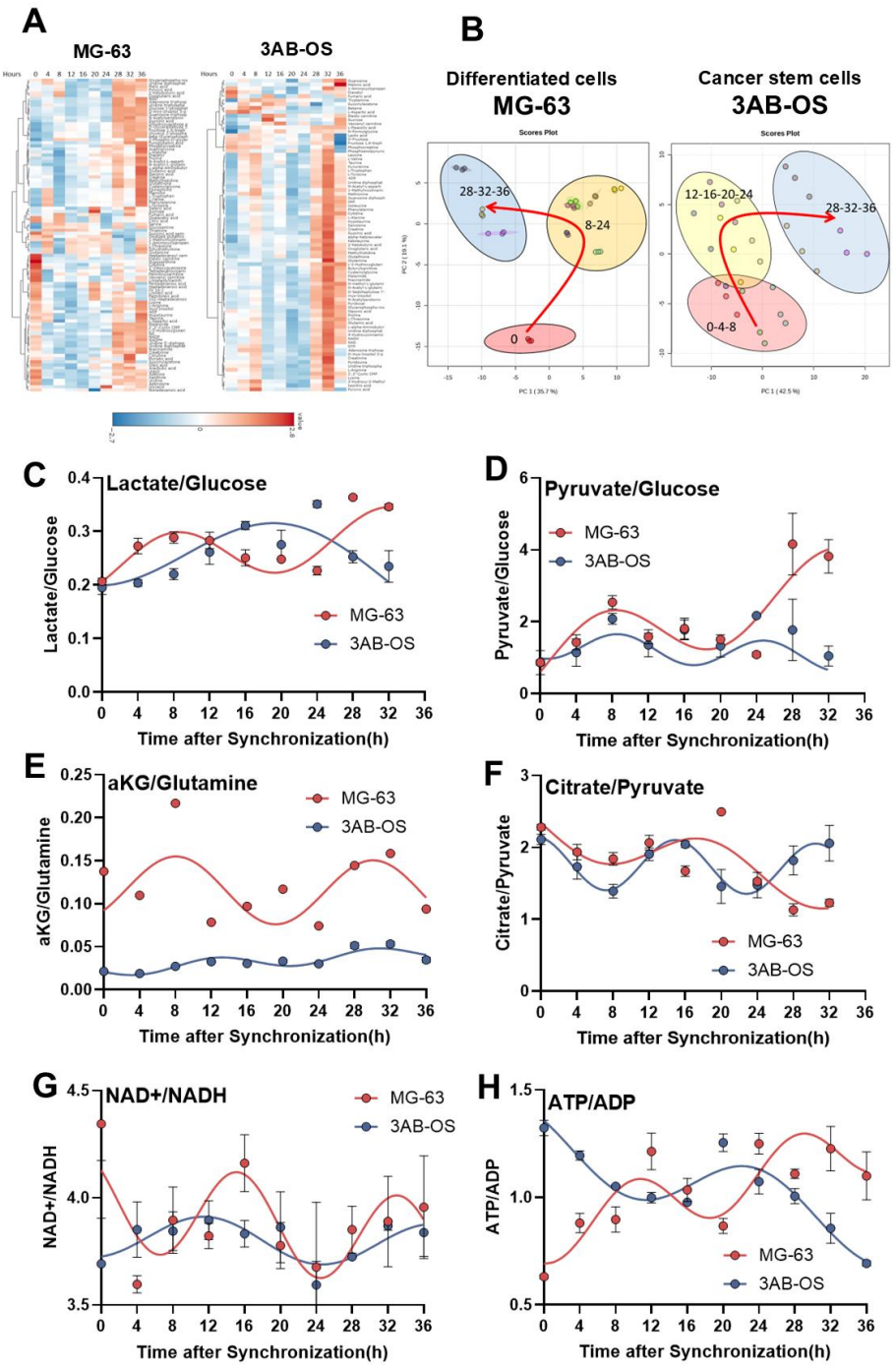

Figure 14. Metabolomic analysis in synchronized DCCs and CSCs. Time-resolved polar metabolites analysis obtained using LC-MS. Heat map (A) showing differential abundance over time of polar metabolites. Principal component analysis (B) of metabolite changing over time. Lactate/Glucose (C), Pyruvate/Glucose (D), aKetoglutarate/Glutamine (E) and Citrate/Pyruvate (F) ratios where dots show mean±SEM, continuous line shows Cosinor best fitting curve. NAD+/NADH (G) and ATP/ADP (H) ratios where dots show mean±SEM, continuous line shows Cosinor best fitting curve.

4.8 Discussion

The role of circadian rhythms has become a topic of increasing interest in the cancer field, since many of the cancer hallmarks are known to be controlled by the molecular clockwork[2]. Moreover, cancer stem cells are a hot research topic for their prominent role in oncogenesis and drug resistance, being the root of intra-tumor heterogeneity and considered one of the main root causes of treatment failure and disease relapse. In the last years there have been numerous reports about circadian rhythms being suppressed in stem cells, and in particular in cancer stem cells, where it has been demonstrated how molecular clock alterations can have a role in maintenance of self-renewal and stemness potential[22].

In this context, our study wants to fill in the gap between circadian rhythms role in the regulation of CSCs regarding their metabolic rewiring, proliferative potential and drug resistance. Starting from the knowledge that clock gene can act as tumour suppressor or oncogenes depending on different cancer types[94,95], we first characterized the circadian phenotype several cancer models using real-time luciferase activity assay of lentivirally transduced cells with a pBMAL1::luc construct, finding a dampened rhythmic profile of Bmal1 promoter activation in bladder cancer and osteosarcoma CSCs when compared to the differentiated counterpart, which in contrast showed robust circadian oscillations. In breast cancer differentiated cells there was a slow clockwork response to the synchronization stimulus, with the first positive peak around 36 hours, meanwhile in MDA stem-like cells the oscillation was lost rather quickly. We confirmed previous observations that reported reduced or absent oscillations in CSCs[22], while in DCCs circadian function is robust, although phenotypes can vary depending on the cancer type.

We next focused on the tumour bulk-cancer stem sub-clone dichotomy choosing to deepen the molecular characterization of the osteosarcoma model, composed by MG-63 differentiated cells and 3AB-OS cancer stem cells derived from long term exposure of MG-63 to 3-aminobenzamide[104], which have also been extensively studied regarding

their metabolism and drug resistance[110,111]. The CSCs circadian deregulation was also confirmed at the mRNA, where clock master regulator Bmal1 and Rev-Erbα rhythmic profile present in MG-63 were abolished in 3AB-OS cells. Protein expression of Bmal1 was also found to be reduced in CSCs, while Rev-Erbα was upregulated despite the reduced mRNA levels previously observed. We speculated that Rev-Erbα protein degradation rates could be reduced, leading to accumulation of the protein even in a setting of low transcript levels. This could then lead to Bmal1 transcript and protein downregulation. The upregulation of c-myc could also be a strategy that CSCs adopt to keep Bmal1 protein levels reduced via promoting Rev-Erbα transcription and upregulation, as it is reported in other osteosarcoma cells[70], although in our model Rev-Erbα transcript levels are low, suggesting that this could be a less likely explanation. In turn c-myc can also directly repress Bmal1 transcription[71], which in our case would explain the reduced Bmal1 mRNA and protein expression, that would see as a consequence the reduced mRNA expression of Rev-Erbα. Hence, a slower degradation rate would still be a probable explanation for the increased Rev-Erbα protein levels. In synchronized conditions however CSCs rhythmicity in both Bmal1 and Rev-Erbα was reduced, in accordance with transcript expression analysis.

We therefore successfully achieved our first aim by characterising the circadian phenotype of osteosarcoma DCCs and CSCs, finding similar results already present in literature that indicate the dampening or absence of canonical oscillations in Core Clock Genes expression in stem-subclones deriving from tumor bulk[93].

We then investigated whether the circadian deregulation could have an impact on cell proliferation. We confirmed a higher proliferative potential showed by 3AB-OS compared to MG-63, in accordance with previous evidences reporting strong proliferative a sphere-forming capabilities of these CSCs[104]. By using real-time, high-resolution impedentiomentric measurements, we were able to appreciate a robust variation over time in the proliferation rate of clock-functioning MG-63 cells. In contrast in clock-deficient 3AB-OS cells the proliferative rate

followed a flat profile, and the circadian oscillation was completely abolished. Literature indicates Rev-Erbα as a pro-proliferation agent due to its negative regulation of cell cycle inhibitor p21[62]; in turn Bmal1 is identified as a inhibitor of cell proliferation, being it a transcriptional activator of the negative cell cycle regulator kinase Wee-1[61]; 3AB-OS cells also display high levels of cell cycle markers which account for G1-S/G2-M phases progression[104], and we speculate that Rev-Erbα upregulation and Bmal1 suppression could contribute to cell cycle progression and enhanced cell proliferation observed in 3AB-OS. The lack of oscillations in the two main core clock genes involved in cell cycle regulation is also reflected in a flat profile of the proliferative rate found in 3AB-OS cells. Pharmacological induction of Bmal1, obtained through Rorα induction, combined with Rev-Erbα inhibition, resulted in a marked cytotoxic effect in MG-63 cells. The inhibition the secondary feedback protein could result in increased p21 expression, while contextual Bmal1 induction could lead to a strong and lethal cell cycle arrest stimulus. We therefore identified clockwork modulation as a valuable strategy in order to impact cell proliferation in DCCs.

The same effect however was not observed in 3AB-OS cancer stem cells, where combined treatment was not able to achieve a significant Bmal1 mRNA and protein levels increase, and only saw a modest and non-significant reduction of cell proliferation. It has been reported in the past that 3AB-OS are drug-resistant cells due to efflux pump ABCG2 expression[104], and we cannot exclude that treatment failure can be attributed to drug expulsion or detoxification. We could also speculate that the lack of clock function and especially Bmal1 reduced expression, is functional in 3AB-OS to remove the circadian control on cell growth, conferring a proliferative advantage and insensitivity to exogenous circadian-stimuli to 3AB-OS cells. This could be a mechanism by which a stem-subclone is selected in the tumor bulk: by having a deregulation of cellular clock, CSCs are unresponsive to external entrainment cues exerted by the central clock, and can thereby escape the circadian control to which

differentiated cancer cells are subjected to in terms of proliferative potential, gaining in this way a fitness advantage among the tumor bulk.

Being metabolic rewiring among cancer hallmarks governed by the clockwork, we then focused on the circadian deregulation effects on metabolic profile of osteosarcoma DCCs and CSCs, as previous reports indicated 3AB-OS as highly glycolytic and metabolically plastic cells[110,111]. Both real time and time-point OCR analysis showed 24h period oscillatory mitochondrial respiration pattern in MG-63, whereas 3AB-OS displayed a longer and deregulated profile and glycolytic activity compensated for OXPHOS. Overall osteosarcoma CSCs lack of circadian regulation confers them a highly plastic phenotype during the different times after synchronization, while DCCs remain constrained in a oxidative phenotype. ATP production reveal a similar scenario, where DCCs draw the majority of the ATP from OXPHOS, while 3AB-OS relay preferentially on glycolytic ATP production over the different time-points. When comparing the metabolic fluxes with time resolved polar metabolites analysis, lactate/glucose ratio, a proxy measurement of the glycolytic flux, revealed a similar oscillatory pattern to the glycolytic activity in CSCs measured with the Seahorse platform. In MG-63 cells α-ketoglutarate/glutamine ratio, used as an indication of glutamine shunt into the TCA cycle, revealed peaks at the same time points of higher mitochondrial respiration, suggesting glutamine oxidation as a likely mitochondrial fuelling pathway in DCCs. This result is consistent with previous works indicating glucose as a prominent substrate used by 3AB-OS, while MG-63 were found to be glutamine-dependent cells[110,111]. Overall the differential selective substrate utilization between the two cell line over time recapitulates their metabolic profile observed in the extracellular metabolic flux analysis and in previous reports.

Future perspectives stemming from this work would be to perform silencing or overexpression studies of Bmal1 and Rev-Erbα in order to confirm and properly dissect the molecular mechanisms that governs the interplay between clock genes, tumorigenesis and CSCs biology.

5 CONCLUSIONS

We successfully characterized the circadian phenotype of several cancer models from a molecular point of view, confirming a deregulation in core clock genes oscillations in CSCs.

We then reported a circadian proliferation profile in clock-functioning DCCs, which was indeed absent in CSCs. We then identified clock modulation as possible strategy to target DCCs proliferation. At the same time we revealed how circadian deregulation can confer an advantage to CSCs in terms of escape from exogenous circadian stimuli.

Finally, we verified how differential circadian phenotype governs cellular bioenergetics, as in DCCs metabolism oscillates in a circadian fashion, while the lack of circadian control allows CSCs to display a higher degree of metabolic plasticity.

Altogether this work contributes to advance the current knowledge on the role of circadian molecular network in cancer heterogeneity, and confirms clock-modulating intervention as a valuable strategies to target tumor vulnerabilities, although more studies are needed to fully elucidate how to combine the use of chronotherapy and conventional chemotherapy to target Cancer Stem Cells.

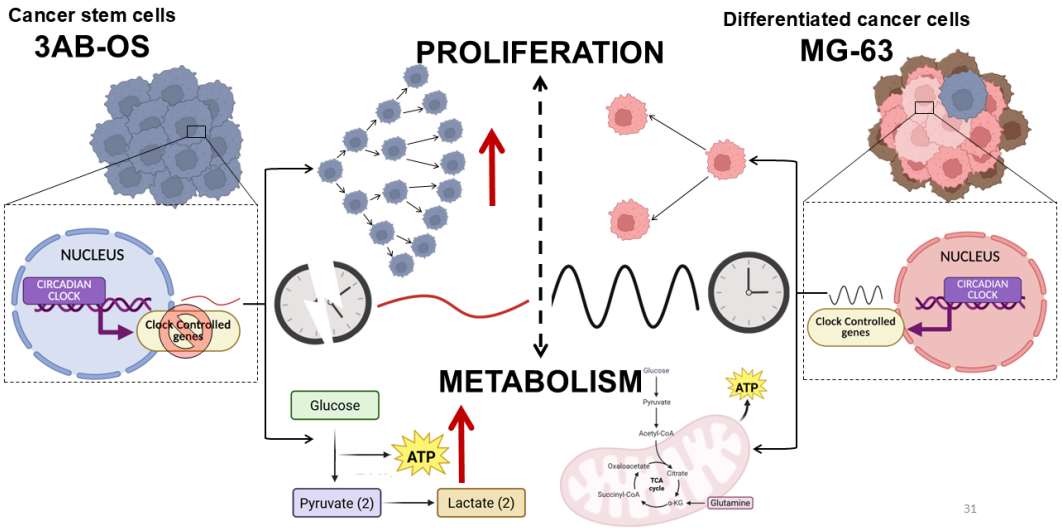

Figure 15. Graphical abstract

6 BIBLIOGRAPHY

1. Lee Y. Roles of circadian clocks in cancer pathogenesis and treatment. *Exp Mol Med*. 2021;53(10):1529-1538. doi:10.1038/s12276-021-00681-0

2. Lian JW, Li SY, Clarke RB, Howell SJ, Meng QJ. Can we utilise the circadian clock to target cancer stem cells? *Cancer Letters*. 2025;611:217360. doi:10.1016/j.canlet.2024.217360

3. Takahashi JS, Hong HK, Ko CH, McDearmon EL. The genetics of mammalian circadian order and disorder: implications for physiology and disease. *Nat Rev Genet*. 2008;9(10):764-775. doi:10.1038/nrg2430

4. Zhu X, Maier G, Panda S. Learning from circadian rhythm to transform cancer prevention, prognosis, and survivorship care. *Trends in Cancer*. 2024;10(3):196-207. doi:10.1016/j.trecan.2023.11.002

5. Abreu M, Basti A, Genov N, Mazzoccoli G, Relógio A. The reciprocal interplay between TNFα and the circadian clock impacts on cell proliferation and migration in Hodgkin lymphoma cells. *Sci Rep*. 2018;8(1):11474. doi:10.1038/s41598-018-29847-z

6. Patke A, Young MW, Axelrod S. Molecular mechanisms and physiological importance of circadian rhythms. *Nat Rev Mol Cell Biol*. 2020;21(2):67-84. doi:10.1038/s41580-019-0179-2

7. Takahashi JS. Transcriptional architecture of the mammalian circadian clock. *Nat Rev Genet*. 2017;18(3):164-179. doi:10.1038/nrg.2016.150

8. Gekakis N, Staknis D, Nguyen HB, et al. Role of the CLOCK Protein in the Mammalian Circadian Mechanism. *Science*. 1998;280(5369):1564-1569. doi:10.1126/science.280.5369.1564

9. Yoo SH, Ko CH, Lowrey PL, et al. A noncanonical E-box enhancer drives mouse *Period2* circadian oscillations *in vivo*. *Proc Natl Acad Sci USA*. 2005;102(7):2608-2613. doi:10.1073/pnas.0409763102

10. Camacho F, Cilio M, Guo Y, et al. Human casein kinase Iδ phosphorylation of human circadian clock proteins period 1 and 2. *FEBS Letters*. 2001;489(2-3):159-165. doi:10.1016/S0014-5793(00)02434-0

11. Eide EJ, Virshup DM. CASEIN KINASE I: ANOTHER COG IN THE CIRCADIAN CLOCKWORKS. *Chronobiology International*. 2001;18(3):389-398. doi:10.1081/CBI-100103963

12. Harada Y, Sakai M, Kurabayashi N, Hirota T, Fukada Y. Ser-557-phosphorylated mCRY2 Is Degraded upon Synergistic Phosphorylation by Glycogen Synthase Kinase-3β. *Journal of Biological Chemistry*. 2005;280(36):31714-31721. doi:10.1074/jbc.M506225200

13. Lamia KA, Sachdeva UM, DiTacchio L, et al. AMPK Regulates the Circadian Clock by Cryptochrome Phosphorylation and Degradation. *Science*. 2009;326(5951):437-440. doi:10.1126/science.1172156

14. Sato TK, Panda S, Miraglia LJ, et al. A Functional Genomics Strategy Reveals Rora as a Component of the Mammalian Circadian Clock. *Neuron*. 2004;43(4):527-537. doi:10.1016/j.neuron.2004.07.018

15. Preitner N, Damiola F, Luis-Lopez-Molina, et al. The Orphan Nuclear Receptor REV-ERBα Controls Circadian Transcription within the Positive Limb of the Mammalian Circadian Oscillator. *Cell*. 2002;110(2):251-260. doi:10.1016/S0092-8674(02)00825-5

16. Zhu B, Liu S, David NL, et al. Evidence for ~12-h ultradian gene programs in humans. *npj Biol Timing Sleep*. 2024;1(1):4. doi:10.1038/s44323-024-00005-1

17. Pittendrigh CS. Circadian rhythms and the circadian organization of living systems. *Cold Spring Harb Symp Quant Biol*. 1960;25:159-184. doi:10.1101/sqb.1960.025.01.015

18. Hattar S, Kumar M, Park A, et al. Central projections of melanopsin-expressing retinal ganglion cells in the mouse. *J Comp Neurol*. 2006;497(3):326-349. doi:10.1002/cne.20970

19. Morin LP. SCN organization reconsidered. *J Biol Rhythms*. 2007;22(1):3-13. doi:10.1177/0748730406296749

20. Alibhai FJ, Tsimakouridze EV, Reitz CJ, Pyle WG, Martino TA. Consequences of Circadian and Sleep Disturbances for the Cardiovascular System. *Can J Cardiol*. 2015;31(7):860-872. doi:10.1016/j.cjca.2015.01.015

21. Grimaldi D, Carter JR, Van Cauter E, Leproult R. Adverse Impact of Sleep Restriction and Circadian Misalignment on Autonomic Function in Healthy Young Adults. *Hypertension*. 2016;68(1):243-250. doi:10.1161/HYPERTENSIONAHA.115.06847

22. Lee Y, Tanggono AS. Potential Role of the Circadian Clock in the Regulation of Cancer Stem Cells and Cancer Therapy. *IJMS*. 2022;23(22):14181. doi:10.3390/ijms232214181

23. Marcheva B, Ramsey KM, Peek CB, Affinati A, Maury E, Bass J. Circadian Clocks and Metabolism. *Handb Exp Pharmacol*. 2013;(217):127-155. doi:10.1007/978-3-642-25950-0_6

24. Neumann AM, Schmidt CX, Brockmann RM, Oster H. Circadian regulation of endocrine systems. *Autonomic Neuroscience*. 2019;216:1-8. doi:10.1016/j.autneu.2018.10.001

25. Fonken LK, Workman JL, Walton JC, et al. Light at night increases body mass by shifting the time of food intake. *Proc Natl Acad Sci U S A*. 2010;107(43):18664-18669. doi:10.1073/pnas.1008734107

26. Marcheva B, Ramsey KM, Buhr ED, et al. Disruption of the clock components CLOCK and BMAL1 leads to hypoinsulinaemia and diabetes. *Nature*. 2010;466(7306):627-631. doi:10.1038/nature09253

27. Turek FW, Joshu C, Kohsaka A, et al. Obesity and metabolic syndrome in circadian Clock mutant mice. *Science*. 2005;308(5724):1043-1045. doi:10.1126/science.1108750

28. Kudo T, Tamagawa T, Kawashima M, Mito N, Shibata S. Attenuating effect of clock mutation on triglyceride contents in the ICR mouse liver under a high-fat diet. *J Biol Rhythms*. 2007;22(4):312-323. doi:10.1177/0748730407302625

29. Shimba S, Ishii N, Ohta Y, et al. Brain and muscle Arnt-like protein-1 (BMAL1), a component of the molecular clock, regulates adipogenesis. *Proc Natl Acad Sci U S A*. 2005;102(34):12071-12076. doi:10.1073/pnas.0502383102

30. McCarthy JJ, Andrews JL, McDearmon EL, et al. Identification of the circadian transcriptome in adult mouse skeletal muscle. *Physiol Genomics*. 2007;31(1):86-95. doi:10.1152/physiolgenomics.00066.2007

31. Lamia KA, Storch KF, Weitz CJ. Physiological significance of a peripheral tissue circadian clock. *Proc Natl Acad Sci U S A*. 2008;105(39):15172-15177. doi:10.1073/pnas.0806717105

32. Carvas JM, Vukolic A, Yepuri G, et al. Period2 gene mutant mice show compromised insulin-mediated endothelial nitric oxide release and altered glucose homeostasis. *Front Physiol*. 2012;3:337. doi:10.3389/fphys.2012.00337

33. Yang S, Liu A, Weidenhammer A, et al. The role of mPer2 clock gene in glucocorticoid and feeding rhythms. *Endocrinology*. 2009;150(5):2153-2160. doi:10.1210/en.2008-0705

34. Zhang EE, Kay SA. Clocks not winding down: unravelling circadian networks. *Nat Rev Mol Cell Biol*. 2010;11(11):764-776. doi:10.1038/nrm2995

35. Baggs JE, Price TS, DiTacchio L, Panda S, Fitzgerald GA, Hogenesch JB. Network features of the mammalian circadian clock. *PLoS Biol*. 2009;7(3):e52. doi:10.1371/journal.pbio.1000052

36. Green CB, Douris N, Kojima S, et al. Loss of Nocturnin, a circadian deadenylase, confers resistance to hepatic steatosis and diet-induced obesity. *Proc Natl Acad Sci U S A*. 2007;104(23):9888-9893. doi:10.1073/pnas.0702448104

37. Osellame LD, Blacker TS, Duchen MR. Cellular and molecular mechanisms of mitochondrial function. *Best Pract Res Clin Endocrinol Metab*. 2012;26(6):711-723. doi:10.1016/j.beem.2012.05.003

38. Westermann B. Mitochondrial fusion and fission in cell life and death. *Nat Rev Mol Cell Biol*. 2010;11(12):872-884. doi:10.1038/nrm3013

39. Koike N, Yoo SH, Huang HC, et al. Transcriptional architecture and chromatin landscape of the core circadian clock in mammals. *Science*. 2012;338(6105):349-354. doi:10.1126/science.1226339

40. Jacobi D, Liu S, Burkewitz K, et al. Hepatic Bmal1 Regulates Rhythmic Mitochondrial Dynamics and Promotes Metabolic Fitness. *Cell Metab*. 2015;22(4):709-720. doi:10.1016/j.cmet.2015.08.006

41. Neufeld-Cohen A, Robles MS, Aviram R, et al. Circadian control of oscillations in mitochondrial rate-limiting enzymes and nutrient utilization by PERIOD proteins. *Proc Natl Acad Sci USA*. 2016;113(12):E1673-1682. doi:10.1073/pnas.1519650113

42. Masri S, Patel VR, Eckel-Mahan KL, et al. Circadian acetylome reveals regulation of mitochondrial metabolic pathways. *Proc Natl Acad Sci U S A*. 2013;110(9):3339-3344. doi:10.1073/pnas.1217632110

43. Peek CB, Affinati AH, Ramsey KM, et al. Circadian clock NAD+ cycle drives mitochondrial oxidative metabolism in mice. *Science*. 2013;342(6158):1243417. doi:10.1126/science.1243417

44. Mauvoisin D, Atger F, Dayon L, et al. Circadian and Feeding Rhythms Orchestrate the Diurnal Liver Acetylome. *Cell Rep*. 2017;20(7):1729-1743. doi:10.1016/j.celrep.2017.07.065

45. Neufeld-Cohen A, Robles MS, Aviram R, et al. Circadian control of oscillations in mitochondrial rate-limiting enzymes and nutrient utilization by PERIOD proteins. *Proc Natl Acad Sci U S A*. 2016;113(12):E1673-1682. doi:10.1073/pnas.1519650113

46. Cela O, Scrima R, Pazienza V, et al. Clock genes-dependent acetylation of complex I sets rhythmic activity of mitochondrial OxPhos. *Biochimica et Biophysica Acta (BBA) - Molecular Cell Research*. 2016;1863(4):596-606. doi:10.1016/j.bbamcr.2015.12.018

47. Hardie DG, Ross FA, Hawley SA. AMPK: a nutrient and energy sensor that maintains energy homeostasis. *Nat Rev Mol Cell Biol*. 2012;13(4):251-262. doi:10.1038/nrm3311

48. Schmitt K, Grimm A, Dallmann R, et al. Circadian Control of DRP1 Activity Regulates Mitochondrial Dynamics and Bioenergetics. *Cell Metabolism*. 2018;27(3):657-666.e5. doi:10.1016/j.cmet.2018.01.011

49. Cela O, Scrima R, Rosiello M, et al. Circadian clockwork controls the balance between mitochondrial turnover and dynamics: What is life … without time marking? *Biochim Biophys Acta Bioenerg*. 2025;1866(2):149542. doi:10.1016/j.bbabio.2025.149542

50. Xu L, Lin J, Liu Y, et al. CLOCK regulates Drp1 mRNA stability and mitochondrial homeostasis by interacting with PUF60. *Cell Rep*. 2022;39(2):110635. doi:10.1016/j.celrep.2022.110635

51. Scrima R, Cela O, Merla G, et al. Clock-genes and mitochondrial respiratory activity: Evidence of a reciprocal interplay. *Biochimica et Biophysica Acta (BBA) - Bioenergetics*. 2016;1857(8):1344-1351. doi:10.1016/j.bbabio.2016.03.035

52. Clemente-Suarez VJ, Navarro-Jiménez E, Benitez-Agudelo JC, et al. The multifaceted impact of circadian disruption on cancer risk: a systematic review of insights and economic implications. *Journal of the National Cancer Center*. 2025;5(5):524-536. doi:10.1016/j.jncc.2025.04.005

53. Ward EM, Germolec D, Kogevinas M, et al. Carcinogenicity of night shift work. *The Lancet Oncology*. 2019;20(8):1058-1059. doi:10.1016/S1470-2045(19)30455-3

54. Hua H, Wang Y, Wan C, et al. Circadian gene *mPer2* overexpression induces cancer cell apoptosis. *Cancer Science*. 2006;97(7):589-596. doi:10.1111/j.1349-7006.2006.00225.x

55. Gong X, Tang H, Yang K. PER1 suppresses glycolysis and cell proliferation in oral squamous cell carcinoma via the PER1/RACK1/PI3K signaling complex. *Cell Death Dis*. 2021;12(3):276. doi:10.1038/s41419-021-03563-5

56. Chan AB, Huber AL, Lamia KA. Cryptochromes modulate E2F family transcription factors. *Sci Rep*. 2020;10(1):4077. doi:10.1038/s41598-020-61087-y

57. Ye Y, Xiang Y, Ozguc FM, et al. The Genomic Landscape and Pharmacogenomic Interactions of Clock Genes in Cancer Chronotherapy. *Cell Syst*. 2018;6(3):314-328.e2. doi:10.1016/j.cels.2018.01.013

58. Wang J, Li S, Li X, et al. Circadian protein BMAL1 promotes breast cancer cell invasion and metastasis by up-regulating matrix metalloproteinase9 expression. *Cancer Cell Int*. 2019;19:182. doi:10.1186/s12935-019-0902-2

59. Lee JH, Gaddameedhi S, Ozturk N, Ye R, Sancar A. DNA damage-specific control of cell death by cryptochrome in p53-mutant ras-transformed cells. *Cancer Res*. 2013;73(2):785-791. doi:10.1158/0008-5472.CAN-12-1994

60. Jia M, Su B, Mo L, et al. Circadian clock protein CRY1 prevents paclitaxel-induced senescence of bladder cancer cells by promoting p53 degradation. *Oncol Rep*. 2021;45(3):1033-1043. doi:10.3892/or.2020.7914

61. Matsuo T, Yamaguchi S, Mitsui S, Emi A, Shimoda F, Okamura H. Control mechanism of the circadian clock for timing of cell division in vivo. *Science*. 2003;302(5643):255-259. doi:10.1126/science.1086271

62. Gréchez-Cassiau A, Rayet B, Guillaumond F, Teboul M, Delaunay F. The Circadian Clock Component BMAL1 Is a Critical Regulator of p21 Expression and Hepatocyte Proliferation. *Journal of Biological Chemistry*. 2008;283(8):4535-4542. doi:10.1074/jbc.M705576200

63. Kang TH, Leem SH. Modulation of ATR-mediated DNA damage checkpoint response by cryptochrome 1. *Nucleic Acids Research*. 2014;42(7):4427-4434. doi:10.1093/nar/gku094

64. Im JS, Jung BH, Kim SE, Lee KH, Lee JK. Per3, a circadian gene, is required for Chk2 activation in human cells. *FEBS Letters*. 2010;584(23):4731-4734. doi:10.1016/j.febslet.2010.11.003

65. Gery S, Komatsu N, Baldjyan L, Yu A, Koo D, Koeffler HP. The Circadian Gene Per1 Plays an Important Role in Cell Growth and DNA Damage Control in Human Cancer Cells. *Molecular Cell*. 2006;22(3):375-382. doi:10.1016/j.molcel.2006.03.038

66. Miki T, Matsumoto T, Zhao Z, Lee CC. p53 regulates Period2 expression and the circadian clock. *Nat Commun*. 2013;4(1):2444. doi:10.1038/ncomms3444

67. Gotoh T, Vila-Caballer M, Santos CS, Liu J, Yang J, Finkielstein CV. The circadian factor Period 2 modulates p53 stability and transcriptional activity in unstressed cells. Solomon MJ, ed. *MBoC*. 2014;25(19):3081-3093. doi:10.1091/mbc.e14-05-0993

68. Liu Z, Selby CP, Yang Y, et al. Circadian regulation of c-MYC in mice. *Proc Natl Acad Sci USA*. 2020;117(35):21609-21617. doi:10.1073/pnas.2011225117

69. Huber AL, Papp SJ, Chan AB, et al. CRY2 and FBXL3 Cooperatively Degrade c-MYC. *Molecular Cell*. 2016;64(4):774-789. doi:10.1016/j.molcel.2016.10.012

70. Altman BJ, Hsieh AL, Sengupta A, et al. MYC Disrupts the Circadian Clock and Metabolism in Cancer Cells. *Cell Metabolism*. 2015;22(6):1009-1019. doi:10.1016/j.cmet.2015.09.003

71. Shostak A, Ruppert B, Ha N, et al. MYC/MIZ1-dependent gene repression inversely coordinates the circadian clock with cell cycle and proliferation. *Nat Commun*. 2016;7:11807. doi:10.1038/ncomms11807

72. Prasetyanti PR, Medema JP. Intra-tumor heterogeneity from a cancer stem cell perspective. *Mol Cancer*. 2017;16(1):41. doi:10.1186/s12943-017-0600-4

73. Cabrera MC, Hollingsworth RE, Hurt EM. Cancer stem cell plasticity and tumor hierarchy. *World J Stem Cells*. 2015;7(1):27-36. doi:10.4252/wjsc.v7.i1.27

74. Reya T, Morrison SJ, Clarke MF, Weissman IL. Stem cells, cancer, and cancer stem cells. *Nature*. 2001;414(6859):105-111. doi:10.1038/35102167

75. Li Y, Laterra J. Cancer Stem Cells: Distinct Entities or Dynamically Regulated Phenotypes? *Cancer Research*. 2012;72(3):576-580. doi:10.1158/0008-5472.CAN-11-3070

76. Marzagalli M, Fontana F, Raimondi M, Limonta P. Cancer Stem Cells—Key Players in Tumor Relapse. *Cancers*. 2021;13(3):376. doi:10.3390/cancers13030376

77. Cruz MH, Sidén Å, Calaf GM, Delwar ZM, Yakisich JS. The Stemness Phenotype Model. *ISRN Oncology*. 2012;2012:1-10. doi:10.5402/2012/392647

78. Chu X, Tian W, Ning J, et al. Cancer stem cells: advances in knowledge and implications for cancer therapy. *Sig Transduct Target Ther*. 2024;9(1):170. doi:10.1038/s41392-024-01851-y

79. Hass R, von der Ohe J, Ungefroren H. Impact of the Tumor Microenvironment on Tumor Heterogeneity and Consequences for Cancer Cell Plasticity and Stemness. *Cancers (Basel)*. 2020;12(12):3716. doi:10.3390/cancers12123716

80. Walcher L, Kistenmacher AK, Suo H, et al. Cancer Stem Cells—Origins and Biomarkers: Perspectives for Targeted Personalized Therapies. *Front Immunol*. 2020;11:1280. doi:10.3389/fimmu.2020.01280

81. Wen GM, Xu XY, Xia P. Metabolism in Cancer Stem Cells: Targets for Clinical Treatment. *Cells*. 2022;11(23):3790. doi:10.3390/cells11233790

82. Johar D, Elmehrath AO, Khalil RM, et al. Protein networks linking Warburg and reverse Warburg effects to cancer cell metabolism. *Biofactors*. 2021;47(5):713-728. doi:10.1002/biof.1768

83. Warburg O, Wind F, Negelein E. THE METABOLISM OF TUMORS IN THE BODY. *Journal of General Physiology*. 1927;8(6):519-530. doi:10.1085/jgp.8.6.519

84. Abad E, Samino S, Yanes O, Potesil D, Zdrahal Z, Lyakhovich A. Activation of glycogenolysis and glycolysis in breast cancer stem cell models. *Biochimica et Biophysica Acta (BBA) - Molecular Basis of Disease*. 2020;1866(10):165886. doi:10.1016/j.bbadis.2020.165886

85. Dual-targeting of aberrant glucose metabolism in glioblastoma - PubMed. Accessed November 12, 2025. https://pubmed.ncbi.nlm.nih.gov/25652202/

86. Michelakis ED, Sutendra G, Dromparis P, et al. Metabolic modulation of glioblastoma with dichloroacetate. *Sci Transl Med*. 2010;2(31):31ra34. doi:10.1126/scitranslmed.3000677

87. Yang Y, Karakhanova S, Hartwig W, et al. Mitochondria and Mitochondrial ROS in Cancer: Novel Targets for Anticancer Therapy. *Journal of Cellular Physiology*. 2016;231(12):2570-2581. doi:10.1002/jcp.25349

88. Zhong G, Qin S, Townsend D, Schulte BA, Tew KD, Wang GY. Oxidative stress induces senescence in breast cancer stem cells. *Biochem Biophys Res Commun*. 2019;514(4):1204-1209. doi:10.1016/j.bbrc.2019.05.098

89. Qu Q, Zeng F, Liu X, Wang QJ, Deng F. Fatty acid oxidation and carnitine palmitoyltransferase I: emerging therapeutic targets in cancer. *Cell Death Dis*. 2016;7(5):e2226-e2226. doi:10.1038/cddis.2016.132

90. Umemura Y, Koike N, Matsumoto T, et al. Transcriptional program of Kpna2/Importin-α2 regulates cellular differentiation-coupled circadian clock development in mammalian cells. *Proceedings of the National Academy of Sciences*. 2014;111(47):E5039-E5048. doi:10.1073/pnas.1419272111

91. Agriesti F, Cela O, Capitanio N. “Time Is out of Joint” in Pluripotent Stem Cells: How and Why. *Int J Mol Sci*. 2024;25(4):2063. doi:10.3390/ijms25042063

92. De A, Beligala DH, Sharma VP, Burgos CA, Lee AM, Geusz ME. Cancer stem cell generation during epithelial-mesenchymal transition is temporally gated by intrinsic circadian clocks. *Clin Exp Metastasis*. 2020;37(5):617-635. doi:10.1007/s10585-020-10051-1

93. Matsunaga N, Ogino T, Hara Y, Tanaka T, Koyanagi S, Ohdo S. Optimized Dosing Schedule Based on Circadian Dynamics of Mouse Breast Cancer Stem Cells Improves the Antitumor Effects of Aldehyde Dehydrogenase Inhibitor. *Cancer Res*. 2018;78(13):3698-3708. doi:10.1158/0008-5472.CAN-17-4034

94. Ogino T, Matsunaga N, Tanaka T, et al. Post-transcriptional repression of circadian component CLOCK regulates cancer-stemness in murine breast cancer cells. Liu C, Zaidi M, Liu C, eds. *eLife*. 2021;10:e66155. doi:10.7554/eLife.66155

95. Dong Z, Zhang G, Qu M, et al. Targeting Glioblastoma Stem Cells through Disruption of the Circadian Clock. *Cancer Discovery*. 2019;9(11):1556-1573. doi:10.1158/2159-8290.CD-19-0215

96. Balsalobre A, Damiola F, Schibler U. A serum shock induces circadian gene expression in mammalian tissue culture cells. *Cell*. 1998;93(6):929-937. doi:10.1016/s0092-8674(00)81199-x

97. Balsalobre A, Marcacci L, Schibler U. Multiple signaling pathways elicit circadian gene expression in cultured Rat-1 fibroblasts. *Curr Biol*. 2000;10(20):1291-1294. doi:10.1016/s0960-9822(00)00758-2

98. Ferrante A, Tamma M, Agriesti F, et al. Characterization of the effect of pomegranate crude extract, and its post-harvesting preservation procedures, on redox tone, cellular growth and metabolic profile of MDA-MB-231 cell line. *BMC Complementary Medicine and Therapies*. 2023;23(1):311. doi:10.1186/s12906-023-04134-1

99. Cornelissen G. Cosinor-based rhythmometry. *Theoretical Biology and Medical Modelling*. 2014;11(1):16. doi:10.1186/1742-4682-11-16

100. Rigby CC, Franks LM. A human tissue culture cell line from a transitional cell tumour of the urinary bladder: growth, chromosone pattern and ultrastructure. *Br J Cancer*. 1970;24(4):746-754. doi:10.1038/bjc.1970.89

101. Bubeník J, Baresová M, Viklický V, Jakoubková J, Sainerová H, Donner J. Established cell line of urinary bladder carcinoma (T24) containing tumour-specific antigen. *Int J Cancer*. 1973;11(3):765-773. doi:10.1002/ijc.2910110327

102. Zhang R, Xia J, Wang Y, et al. Co-Expression of Stem Cell and Epithelial Mesenchymal Transition Markers in Circulating Tumor Cells

of Bladder Cancer Patients. *Onco Targets Ther*. 2020;13:10739-10748. doi:10.2147/OTT.S259240

103. Kim CJ, Terado T, Tambe Y, et al. Anti-oncogenic activities of cyclin D1b siRNA on human bladder cancer cells via induction of apoptosis and suppression of cancer cell stemness and invasiveness. *International Journal of Oncology*. 2018;52(1):231-240. doi:10.3892/ijo.2017.4194

104. Di Fiore R, Santulli A, Drago Ferrante R, et al. Identification and expansion of human osteosarcoma-cancer-stem cells by long-term 3-aminobenzamide treatment. *Journal of Cellular Physiology*. 2009;219(2):301-313. doi:10.1002/jcp.21667

105. Horwitz KB, Costlow ME, McGuire WL. MCF-7; a human breast cancer cell line with estrogen, androgen, progesterone, and glucocorticoid receptors. *Steroids*. 1975;26(6):785-795. doi:10.1016/0039-128x(75)90110-5

106. Vantangoli MM, Madnick SJ, Huse SM, Weston P, Boekelheide K. MCF-7 Human Breast Cancer Cells Form Differentiated Microtissues in Scaffold-Free Hydrogels. *PLoS One*. 2015;10(8):e0135426. doi:10.1371/journal.pone.0135426

107. Wanandi SI, Syahrani RA, Arumsari S, Wideani G, Hardiany NS. Profiling of Gene Expression Associated with Stemness and Aggressiveness of ALDH1A1-Expressing Human Breast Cancer Cells. *Malays J Med Sci*. 2019;26(5):38-52. doi:10.21315/mjms2019.26.5.4

108. Dai X, Cheng H, Bai Z, Li J. Breast Cancer Cell Line Classification and Its Relevance with Breast Tumor Subtyping. *J Cancer*. 2017;8(16):3131-3141. doi:10.7150/jca.18457

109. Fuhr L, El-Athman R, Scrima R, et al. The Circadian Clock Regulates Metabolic Phenotype Rewiring Via HKDC1 and Modulates Tumor Progression and Drug Response in Colorectal Cancer. *EBioMedicine*. 2018;33:105-121. doi:10.1016/j.ebiom.2018.07.002

110. Palorini R, Votta G, Balestrieri C, et al. Energy Metabolism Characterization of a Novel Cancer Stem Cell-Like Line 3AB-OS. *Journal of Cellular Biochemistry*. 2014;115(2):368-379. doi:10.1002/jcb.24671

111. Della Sala G, Pacelli C, Agriesti F, et al. Unveiling Metabolic Vulnerability and Plasticity of Human Osteosarcoma Stem and Differentiated Cells to Improve Cancer Therapy. *Biomedicines*. 2021;10(1):28. doi:10.3390/biomedicines10010028

112. You S, Wood PA, Xiong Y, Kobayashi M, Du-Quiton J, Hrushesky WJM. Daily coordination of cancer growth and circadian clock gene

expression. *Breast Cancer Res Treat*. 2005;91(1):47-60. doi:10.1007/s10549-004-6603-z

113. Kiessling S, Beaulieu-Laroche L, Blum ID, et al. Enhancing circadian clock function in cancer cells inhibits tumor growth. *BMC Biology*. 2017;15(1):13. doi:10.1186/s12915-017-0349-7

114. Mookerjee SA, Gerencser AA, Nicholls DG, Brand MD. Quantifying intracellular rates of glycolytic and oxidative ATP production and consumption using extracellular flux measurements. *J Biol Chem*. 2017;292(17):7189-7207. doi:10.1074/jbc.M116.774471

7 ABSTRACTS

The data and findings featured in this thesis were presented at the 5th Workshop of the SIB group "Tumor Biochemistry" held in Turin, June 9-10th 2025, as an oral contribution and at the 63° SIB Congress held in Palermo, 10-12th September 2025, as a poster presentation. Below is the abstract accepted at the conferences.

Featuring circadian metabolism of Cancer Stem and Differentiated Cells to improve cancer therapy

Francesca Agriesti[1], Aristide Ferrante[1], Consiglia Pacelli[1], Simone Serrao[2], Giuseppe Paglia[2], Nazzareno Capitanio[1], Claudia Piccoli[1]

1 Department of Clinical and Experimental Medicine University of Foggia; francesca.agriesti@unifg.it; aristide.ferrante@unifg.it; consiglia.pacelli@unifg.it; nazzareno.capitanio@unifg.it,; claudia.piccoli@unifg.it

2 Proteomics and Metabolomics units, School of Medicine and Surgery University of Milano-Bicocca; simone.serrao@unimib.it, giuseppe.paglia@unimib.it

Background and aims

An intricate interplay between the circadian clock, oncogenesis, and metabolism is emerging. Circadian disruption and metabolic rewiring are closely linked in cancer, affecting tumour growth, drug resistance, and patient outcomes. In cancer stem cells (CSCs), circadian dysregulation may modulate differentiation and chemoresistance. This study aimed to investigate how circadian rhythm alterations affect metabolism and contribute to CSC survival and drug response, uncovering potential therapeutic vulnerabilities.

Methods

CSCs and differentiated cells from bladder, breast, and osteosarcoma models were lentivirally transduced with a BMAL1 promoter-driven luciferase construct [1]. Live-cell bioluminescence of in vitro synchronized cultures was recorded continuously for 72 h using LumiCycle. Real-time basal oxygen consumption was monitored via Resipher®. Seahorse analysis was used for metabolic flux profiling. Protein and gene expression of clock

components were assessed by western blot and qRT-PCR. Targeted metabolomics was performed using UHPLC coupled with Q-Trap MS [2].

Results

Bioluminescence analysis revealed divergent circadian phenotypes: differentiated cells showed robust rhythms, while CSCs displayed impaired oscillations. Similarly, although all cell types exhibited rhythmic mitochondrial respiration, CSCs showed markedly dampened oscillations, correlating with reduced expression of Bmal1 and other core clock genes. Time-resolved metabolomic profiling of synchronized cultures revealed distinct circadian metabolic dynamics between CSCs and differentiated cells, suggesting identity-specific clock-regulated metabolic programs.

Conclusions

Our findings confirm altered circadian metabolic control in CSCs, likely contributing to their chemoresistance. These insights support the need for chronotype-tailored therapeutic strategies in oncology.

[1] Fuhr L et al. EBioMedicine. 2018 ;33:105-121.
[2] Paglia G, Astarita G. Methods Mol Biol. 2022;2396:137-159.